1741

File copy

ARBRL-CR-00358

BRL

ADA052303

CONTRACT REPORT ARBRL-CR-00358

MODELING OF THE UH-1B TAIL BOOM FOR ANALYSIS BY THE NASTRAN COMPUTER PROGRAM

Prepared by

Kaman AviDyne
A Division of Kaman Sciences Corp
Burlington, Massachusetts 01803

February 1978

Approved for public release; distribution unlimited.

USA ARMAMENT RESEARCH AND DEVELOPMENT COMMAND
USA BALLISTIC RESEARCH LABORATORY
ABERDEEN PROVING GROUND, MARYLAND

UNCLASSIFIED

SECURITY CLASSIFICATION OF THIS PAGE (When Data Entered)

REPORT DOCUMENTATION PAGE

READ INSTRUCTIONS BEFORE COMPLETING FORM

1. REPORT NUMBER: CONTRACT REPORT ARBRL-CR-00358	2. GOVT ACCESSION NO.
3. RECIPIENT'S CATALOG NUMBER	
4. TITLE (and Subtitle): Modeling of the UH-1B Tail Boom for Analysis by the NASTRAN Computer Program	5. TYPE OF REPORT & PERIOD COVERED: Final Report - 19 April 1976 to 19 October 1976
	6. PERFORMING ORG. REPORT NUMBER: KA TR-139
7. AUTHOR(s): Raffi P. Yeghiayan	8. CONTRACT OR GRANT NUMBER(s): DAAD05-76-C-0763
9. PERFORMING ORGANIZATION NAME AND ADDRESS: Kaman AviDyne, A Division of Kaman Sciences Corp., Burlington, Massachusetts 01803	10. PROGRAM ELEMENT, PROJECT, TASK AREA & WORK UNIT NUMBERS
11. CONTROLLING OFFICE NAME AND ADDRESS: US Army Armament Research and Development Command, US Army Ballistic Research Laboratory, (ATTN: DRDAR-BL), Aberdeen Proving Ground, MD 21005	12. REPORT DATE: FEBRUARY 1978
	13. NUMBER OF PAGES: 40
14. MONITORING AGENCY NAME & ADDRESS (if different from Controlling Office)	15. SECURITY CLASS. (of this report): UNCLASSIFIED
	15a. DECLASSIFICATION/DOWNGRADING SCHEDULE

16. DISTRIBUTION STATEMENT (of this Report)

Approved for public release; distribution unlimited.

17. DISTRIBUTION STATEMENT (of the abstract entered in Block 20, if different from Report)

18. SUPPLEMENTARY NOTES

19. KEY WORDS (Continue on reverse side if necessary and identify by block number)

Structural Dynamics
Helicopter Vulnerability
Blast Response
Thermal Response
Nuclear Effects

20. ABSTRACT (Continue on reverse side if necessary and identify by block number)

A representative tail boom of the UH-1B helicopter is modeled for dynamic structural analysis by the NASTRAN computer program. The finite-element model employs beam and plate elements to construct the structural model, which will subsequently be used to study the effects of simulated nuclear detonations, subjecting the model to blast overpressure exposure with and without thermal effects. The lower mode shapes and frequencies of the structural model are generated and presented as a validation check.

DD FORM 1 JAN 73 1473 EDITION OF 1 NOV 65 IS OBSOLETE

UNCLASSIFIED

SECURITY CLASSIFICATION OF THIS PAGE (When Data Entered)

FOREWORD

This report was prepared for the U.S. Army Ballistic Research Laboratory under Contract No. DAAD05-76-C-0763. The Contracting Officer's representative for BRL was Dr. Ennis Quigley.

TABLE OF CONTENTS

LIST OF ILLUSTRATIONS

LIST OF TABLES

I. INTRODUCTION

In recent years, increasing attention has been devoted to the study of structural damage to rotary wing aircraft caused by nuclear weapon detonations. However, the effort has usually been associated with the examination of the effects of separate components of a hostile nuclear environment individually. Thus, blast overpressure damage or thermal exposure damage have been analyzed individually, and the results are acceptable for situations where the interaction between the two environments can be neglected. The combined effects of blast overpressure and thermal exposure may become important when assessing severe damage conditions where the effect of each individual component is of similar magnitude.

The U.S. Army Ballistic Research Laboratory has developed a combined analytical and experimental program to study the combined blast/thermal exposure effects on a UH-1B helicopter tail boom. Kaman AviDyne has participated in this program by developing the finite element structural model of the UH-1B tail boom for analysis by the NASTRAN computer program.

This report presents the details of the data acquisition and modeling assumptions, the finite element structural model developed, and selected results of the natural vibration mode shape and frequency analysis carried out as a validation check of the model. A listing of the input deck is also provided.

II. DATA ACQUISITION AND MODELING ASSUMPTIONS

A major task in the preparation of the UH-1B tail boom finite element structural model was the acquisition and assembling of pertinent data. Many variants of the basic helicopter exist, and the tail boom structure, materials, and assembly also differ from model to model. The desire was to develop a model applicable to two tail booms on hand at BRL and intended for use in the experimental phase of the program. However, the two tail booms were not identical in construction, and documented information on dimensions, weights, section properties and non-structural components pertinent to the particular tail booms on hand were not readily available. The necessary information was gleaned from structural detail drawings obtained at Fort Eustis, Newport News, Virginia, and from some older Bell Helicopter reports and information obtained through private communications. It should be noted, however, that the information assembled did not always apply to the same tail boom, and in some instances did not agree with similar information provided elsewhere.

The finite element structural model was prepared based on the best available data, and from some simplifying assumptions made in developing the model. It will be a relatively simple matter to alter quantities in the input deck if future evaluation and availability of information indicates the necessity of a change from the original model.

The region of interest for analysis and subsequent experiments is the forward section of the tail boom, near the attachment to the helicopter cabin and cargo area section. The tail boom construction consists of bulkhead frames spaced at various distances along tail boom stations and held together via four longerons which are riveted to the bulkhead frames. This space frame is covered by various thicknesses of skin panels which are riveted onto the longeron and bulkhead frame flanges. In addition, the skin panels are stiffened with stringers riveted on them along the length of the tail boom. The stringers are also riveted to the bulkhead frames. Figure 1 depicts the tail boom structure assembly in schematic form.

The bulkhead frames are formed from sheet metal, with a channel cross-sectional shape. Lightening holes are placed at various locations. The bulkhead dimensions decrease in size as the tail boom is tapered down. The four longerons, also formed from sheet metal, lie along straight lines, and define the rounded "corners" of the bulkhead frames. The sheet metal stringers also are along straight lines, and define the conical shape of the tail boom. The uniform cross-sectional shapes of the longerons and stringers are shown in Figure 2, which also shows a sample cross-section of a bulkhead frame.

To accommodate the longerons and stringers, the bulkhead frames have cut-outs at their outer perimeter at the crossing points of the longerons and stringers. Reinforcing gussets are placed to regain some of the stiffness lost due to the cut-outs. Figure 3 shows the detail of a sample bulkhead frame with the cut-outs and locations of the longerons and stringers.

In the finite element model of the above-described structure, the following assumptions are made:

1) The curved shapes of the bulkhead frames are approximated by straight-line segments representing the beam elements.

2) The riveted attachments between longerons and bulkhead frames, also stringers and bulkhead frames, are idealized joints with no relative translational or rotational motion permitted.

3) The cutouts in the bulkhead frames which accommodate the longerons and stringers are ignored, although they represent a serious reduction in the stiffness of the bulkhead frame.

4) The lightening holes are ignored, as they have a minimal effect on the stiffness of the channel-shaped bulkhead frames. The effect of the cutouts on the mass is accounted for as part of the adjustment to the total weight of the tail boom.

5) The complete frame assembly and the attached skin is free of any initial stresses.

6) The curved skin panels are approximated by flat plate elements.

7) The skin panels are ideally joined at their perimeter to the longerons, stringers, or bulkhead frames, with no relative motion permitted.

8) The skin panels are fully active in compression and tension in conjunction with the frame members supporting them; no buckling between rivets is allowed.

The above set of assumptions define some of the modeling simplifications employed. Some of the limitations of the model are implied in the statements of the assumptions. To elaborate on some of the implications, it should be noted that, in reality, when the tail boom is subjected to a force which causes it to bend laterally, the side subjected to tension will have the skin panels contribute to the stiffness only if they are initially taut, otherwise the longerons and stringers will bear the full loading until the skin is pulled taut. Also, the side subjected to compression will not see a contribution from the skin if the skin buckles or is rippled under

compression. Simple calculations show that, if the skin is initially mounted with some slack or is buckled due to the thermal or overpressure effects, the stringers and longerons may reach the yield point in tension before the skin becomes taut enough to be effective and contribute in sharing the load. The conditions will be met for the aluminum frame if the skin has an initial slack of 0.1 inch for a representative span of 21 inches between bulkheads, or when that amount of slack is caused by a temperature rise of 350°F in the skin due to the thermal effects of a nuclear blast (assuming no heating of the shaded frame members).

In addition to the above-listed assumptions which pertain to concepts and are qualitative in nature, some quantitative assumptions were also made concerning the model. Included among the latter are the following assumptions, consecutively numbered:

9) The skin panel thicknesses are the same as specified in Figure 4, and the material is 2024 T3 aluminum alloy, with a modulus of elasticity $E = 10.6 \times 10^6$ psi, and a mass density $\rho = 0.00025$ $\frac{\text{lb sec}^2}{\text{in}^4}$. The UH-1B tail booms available for the test program may have skin panel thicknesses different from the above reference, and it is recommended that samples be physically measured.

10) Beam element properties for all individual bulkheads were assumed to be the same, although some bulkheads obviously have deeper channel-section stems. The assumption of uniformity is justified when one recalls that the relatively stiff bulkheads serve to locate the longerons and stringers, and contribute a negligible amount to the stiffness in lateral bending of the tail boom.

11) All frame members (bulkhead, longerons, and stringers) are made of 7075 T6 aluminum alloy, with a modulus of elasticity

$E = 10.3 \times 10^6$ psi, and a mass density $\rho = 0.00025 \ \frac{\text{lb. sec}^2}{\text{in}^4}$.

12) The coefficient of thermal expansion for all elements is $\alpha = 12.7 \times 10^{-6} \ \frac{\text{in.}}{\text{in.}^\circ\text{F}}$ with a reference room temperature of 70°F.

13) Additional masses to account for hardware and structural and non-structural components not represented in the finite-element model are assumed distributed uniformly along the length of the tail boom, and hence are apportioned at the various stations of the model and represented as lumped masses added at the junction of longerons and bulkhead frames.

Additional details about the modeling approximations are given in the discussion of the finite element structural model developed in the following section.

III. FINITE ELEMENT STRUCTURAL MODEL OF THE UH-1B HELICOPTER TAIL BOOM

The finite element structural model of the UH-1B helicopter tail boom is prepared based on the input requirements of the NASTRAN computer code for dynamic structural analysis. Since the region of interest for the analysis is the forward section of the tail boom, emphasis was placed on modeling that section with greater detail and accuracy, while several justifiable simplifying assumptions were imposed on the aft section of the tail boom and the tail fin.

The structural model is based on the schematic of the UH-1B helicopter tail boom structure shown in Figure 1. Grid points are located at selected intersections of the longerons and stringers with the bulkhead frames. A larger number of grid points are used to model the forward section of the tail boom with greater detail. The aft section and tail fin have fewer grid points and lesser detail. Figure 5 presents the structural grid points and associated grid point numbering sequence, and identifies the global cartesian coordinates employed. The listing of the input deck, attached at the end of this report, gives the coordinates of each grid point in this global axis system (GRID cards in NASTRAN). Grid points are numbered one through 74.

In determining the locations of the grid points, care was taken to insure the collinearity of all grid points lying on the same longeron or stringer. Also, reflective symmetry is assumed about the X-Z vertical plane. It should be noted that all bulkhead frames, except the first one which is the attachment point to the cabin, lie in planes parallel to the Y-Z plane of the global axis system. That first bulkhead frame is tilted at a 6.55 degree angle relative to the Y-Z frame, and grid points 1 through 10 are positioned to reflect that fact. Figure 4.b shows the inclined positioning of the tail boom relative to the cabin.

In addition to the grid points at the attachment bulkhead interface, grid points are located on bulkheads at tail boom stations 17.6, 38.55, 59.50, 80.44, 101.38, and 143.28 inches from the origin. Refer to Figure 1 for the locations of the bulkheads. No grid points are located on bulkheads at tail boom stations 122.23, 164.23, 185.15 and 194.30 for simplification of the model at the aft section of the tail boom. The vertical tail fin is also modeled with the minimum number of grid points feasible.

Figure 6 presents the tail boom model with the beam element identification numbers. The beam elements (CBAR elements in NASTRAN) represent the bulkhead frame, the longeron, and the stringer segments that connect the grid points, and are numbered 101 through 237. The NASTRAN input deck listing at the end of this report shows the CBAR cards, with their identification numbers and reference to the beam property card. Also given are the two grids defining the ends of the

element, and either a third grid point or a set of direction cosines to define the orientation of the cross-sectional properties of the beam element.

Reference to the beam element property cards (PBAR cards in NASTRAN) shows that twenty separate beam elements have been employed, numbered 11 through 30. The basic beam elements are:

PBAR 11 for the stringers

PBAR 12 for the longerons

PBAR 13 for the bulkhead

Beam properties PBAR 20 through 26 represent different combinations of the above, to accommodate elements that are present in the actual tail boom but are not provided for by beam elements in the model. They are instead smeared onto the two adjacent beam elements, whose properties are adjusted to reflect the contribution. The remaining beam element properties (PBAR 14 through 19, and 27 through 30) apply to specific frame members as identified on the CBAR cards.

Each property card represents the result of individual calculations of the properties of a given cross-section, namely the area A, the area moments of inertia I_{yy} and I_{xx}, and the product of inertia J. Table 1 shows the calculation steps involved in determining the above quantities for the basic stringer and longeron cross-sections shown in Figure 2, and Table 2 shows the same calculations for the basic channel cross-section of a bulkhead frame also shown in Figure 2. Similar tedious calculations were also carried out for each of the other beam element property cards.

Figure 7 identifies the plate elements representing the skin panels. The triangular plate elements (CTRIA2 in NASTRAN) are shown with numbers in the 300 series, and the quadrilateral plate elements (CQUAD2 in NASTRAN) are shown with numbers in the 400 series. Note that transition triangular elements 301 through 308 are used to change from a dodecahedron shape at station x = 80.44 in. to the rectangular shape at station x = 101.38 in. As shown in the listing, the triangular elements are referred to property cards (PTRIA2 in NASTRAN) numbered in the thirties, and the quadrilateral elements are referred to property cards (PQUAD2 in NASTRAN) numbered in the forties. The CTRIA2 and CQUAD2 cards also give the set of grid points defining the corners of the plate elements. The property cards indicate the use of four different thickness plates for the model.

The structural model as defined above was used to generate the structural mass matrix of the model. The results are shown in Table 3. Total structural weight amounts to 128 lbs. To bring the total weight in line with the reported 180 lb. weight of the UH-1B tail boom, the balance of 52 lbs. was assumed uniformly distributed along the

227 in. length of the tail boom. This weight may represent hardware such as rivets, gussets, additional structural reinforcements and non-structural components. The 52 lbs. weight was accordingly apportioned along the defined tail boom stations, and the apportioned weight at each station was equally divided between the four grid points representing the junction of the longerons with the bulkhead frames. The listing of the input deck presents these lumped masses (CONM2 cards in NASTRAN) with identification numbers in the 500 series, indicating the grid point number and the magnitude of the mass (in units of $\frac{\text{lb sec}^2}{\text{in}}$) assigned to that grid point. Any discrepancy in the assumed mass distribution may be corrected by adjusting the CONM2 mass values.

The structural model with the added lumped masses was used to generate a new total mass matrix. The results are shown in Table 4, indicating the total weight of 180 lbs.

IV. NATURAL VIBRATION MODE SHAPE AND FREQUENCY ANALYSIS

As a validation check of the finite element structural model of the UH-1B tail boom, the developed model was used in a NASTRAN modal analysis. The input deck employed is listed at the end of this report. The tail boom was assumed rigidly clamped at its attachment interface bulkhead, representing a cantilevered structure. In the subsequent experimental program, the tail booms are intended to be cantilevered from a very heavy steel plate, a condition approaching the above dynamic analysis assumption.

Employing the Givens method of eigenvalue extraction, the NASTRAN results show 192 natural frequencies extracted. The lowest ten natural frequencies are tabulated below:

Mode Number	Frequency (Hz)
1	12.5
2	13.6
3	31.9
4	66.0
5	79.8
6	102.7
7	117.6
8	124.0
9	142.4
10	158.9

Plots of the mode shapes associated with the above natural frequencies were also obtained. The undeformed shape and the first five mode shape plots are presented in Figures 8.a through 8.f.

The undeformed structure is shown in Figure 8.a.

The first mode shape, at a natural frequency of 12.5 Hz is shown in Figure 8.b. The motion represents a lateral first bending mode, with the free end of the tail boom moving alternately in the positive and negative Y-axis directions.

The second mode shape, at a natural frequency of 13.6 Hz. is shown in Figure 8.c. The motion represents the first bending mode in the vertical plane, with the free end of the tail boom moving alternately in the positive and negative Z-axis directions.

The third mode shape, at a natural frequency of 31.9 Hz. is shown in Figure 8.d. The motion represents a twisting mode, where the free end of the tail boom moves in the positive Y-axis direction while the tip of the tail fin moves in the negative Y-axis direction, and vice-versa.

The fourth mode shape, at a natural frequency of 66.0 Hz. is shown in Figure 8.e, and represents the second bending mode in the vertical plane.

The fifth mode shape, at a natural frequency of 79.8 Hz. is shown in Figure 8.f, and represents the second bending mode in the horizontal direction.

V. CONCLUSIONS

The finite element structural model of the UH-1B tail boom was developed based on the available information on the structure dimensions, frame element cross-sections, materials employed, and overall weight.

The assumptions made in developing the simplified model as well as the implied limitations, are enumerated within the report. The modal analysis gives plausible results for the frequencies and mode shapes of the tail boom.

Prior to further use, it is recommended that the model be amended to reflect any improved information on the stiffness contributions of the structural elements or the weight distribution along tail boom stations.

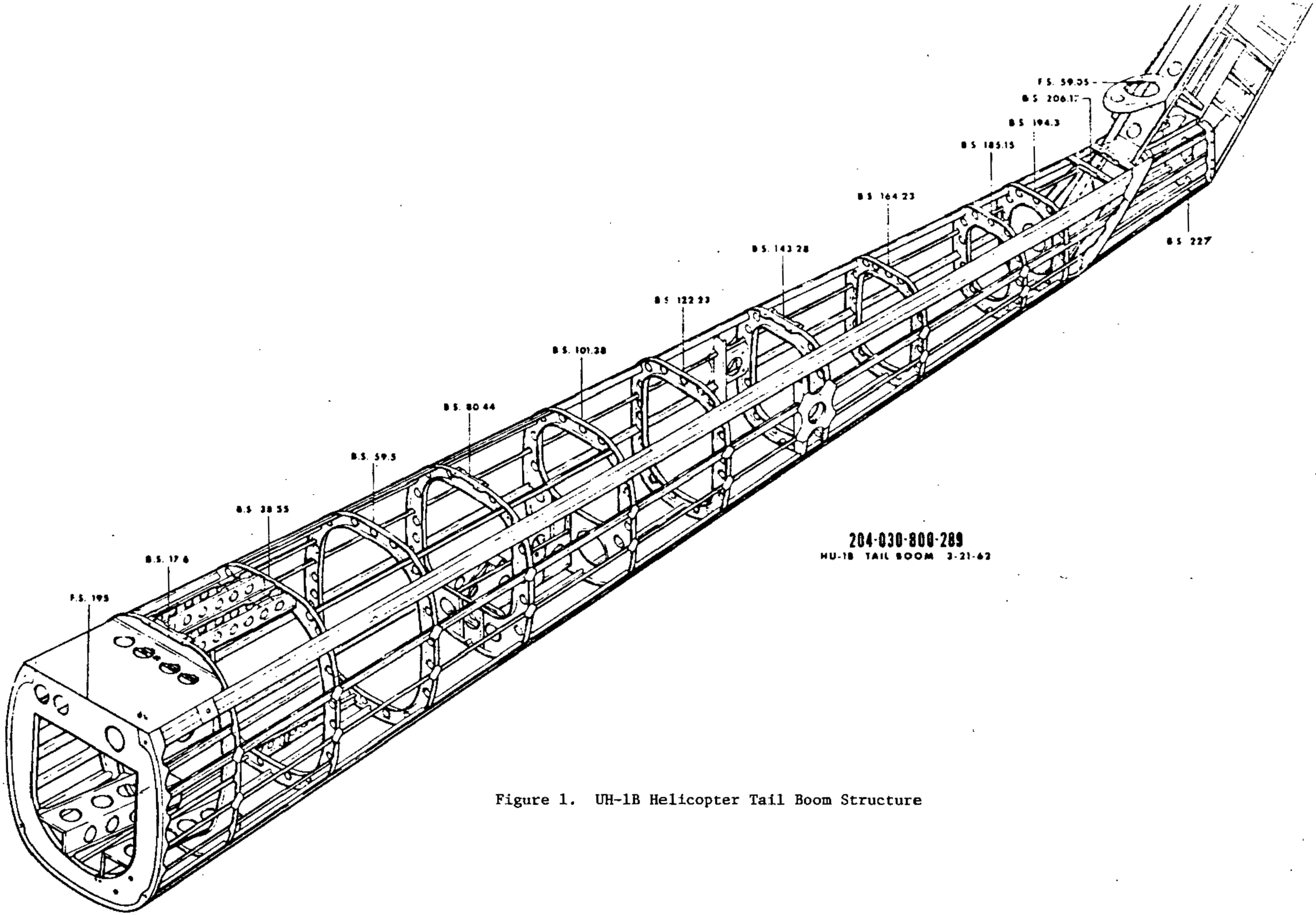

Figure 1. UH-1B Helicopter Tail Boom Structure

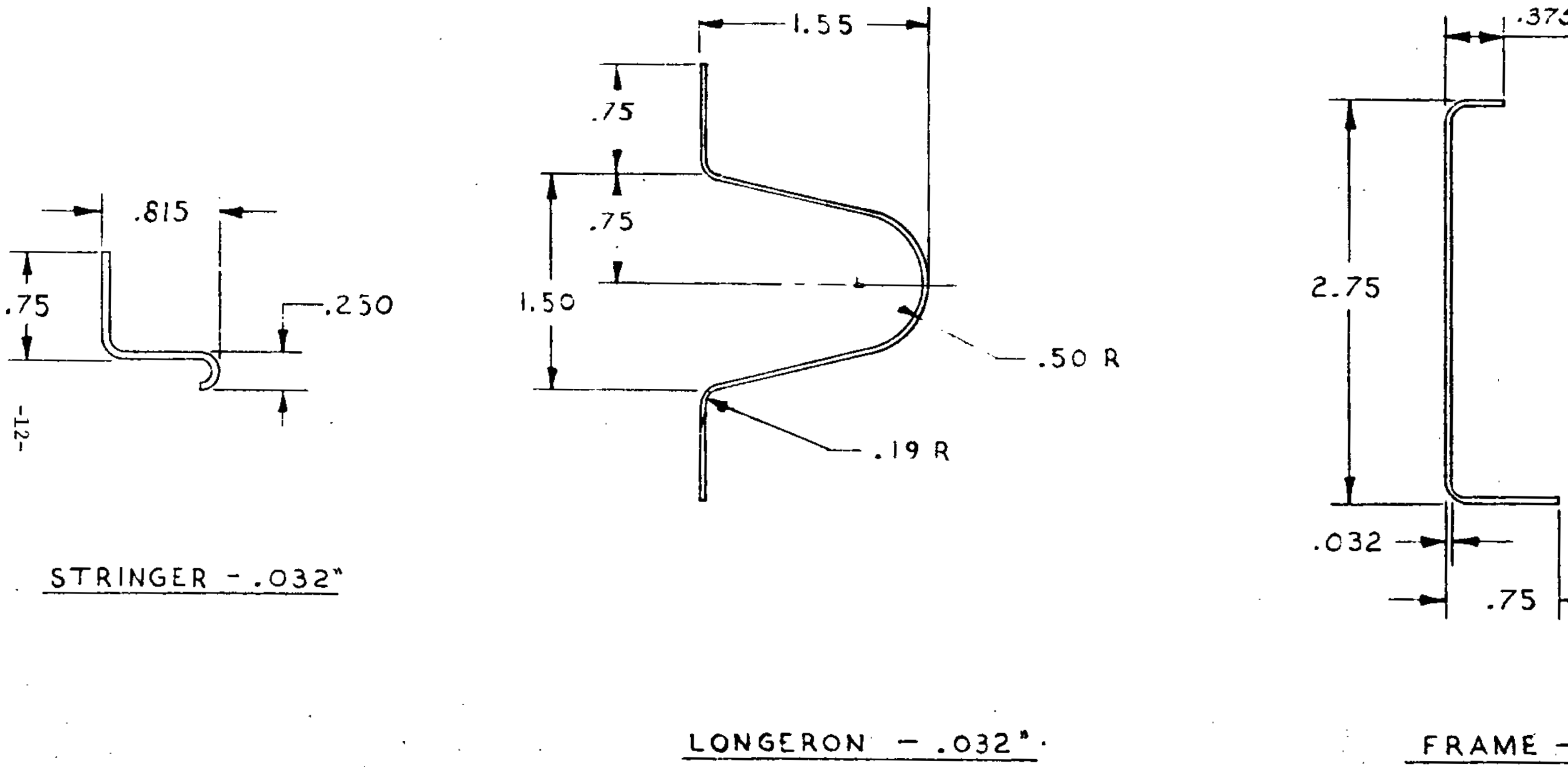

Figure 2. UH-1B Tail Boom Stringer, Longeron, and Bulkhead Frame Cross-Sections

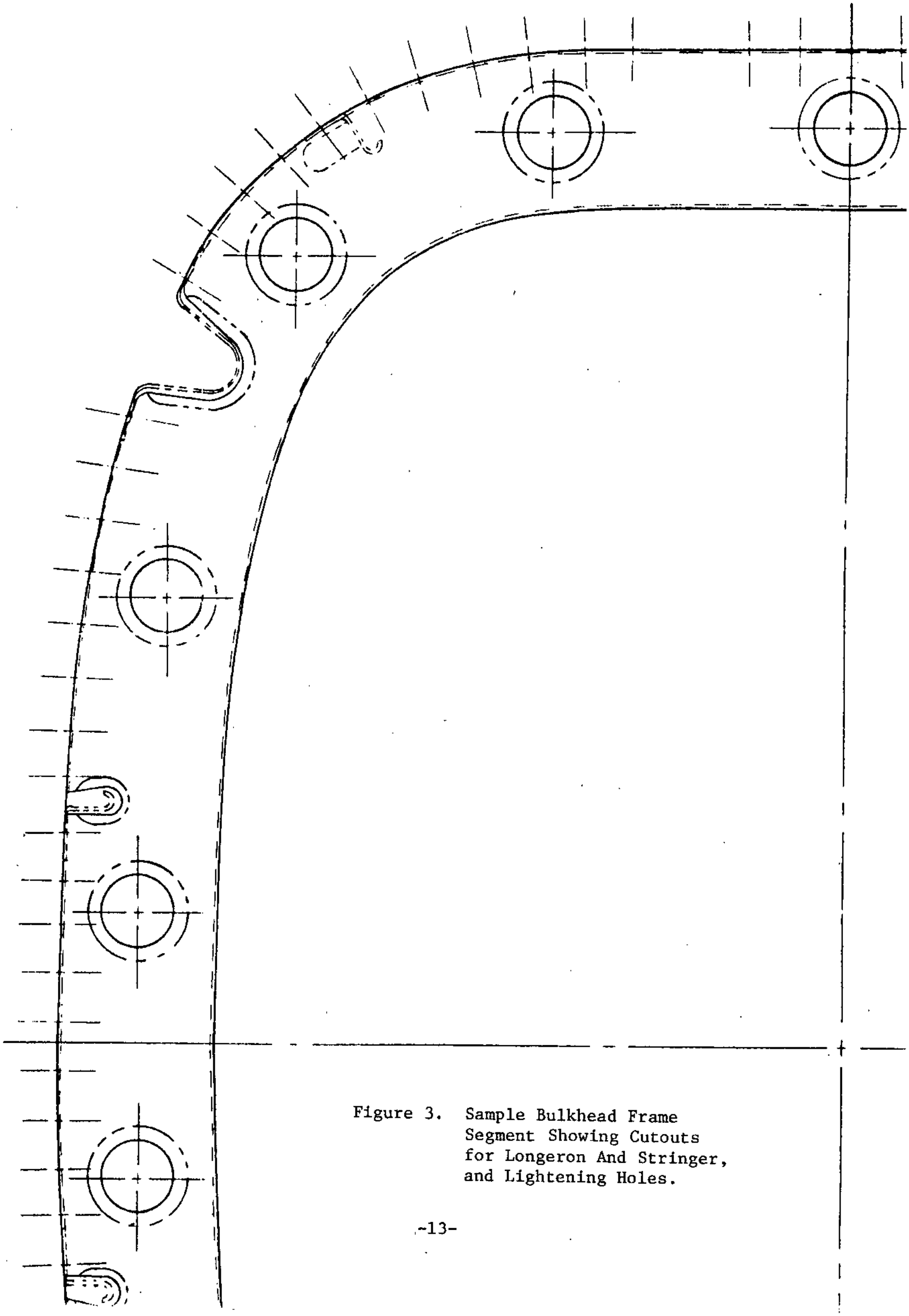

Figure 3. Sample Bulkhead Frame Segment Showing Cutouts for Longeron And Stringer, and Lightening Holes.

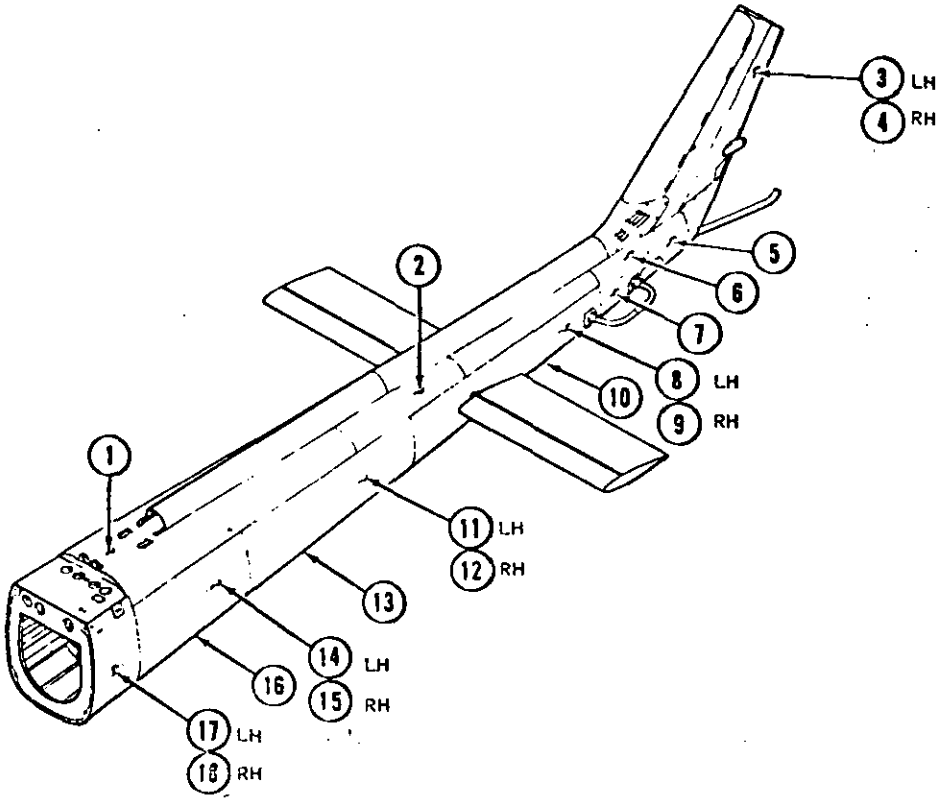

ITEM	MATERIAL	SPECIFICATION	CONDITION	LENGTH	WIDTH	THICKNE
1	Al. Aly	QQ-A-250/5	T3	86.0	40.0	0.020
2	Al. Aly	QQ-A-250/5	T3	96.0	38.0	0.032
3	Al. Aly Faced Honey-comb Panel	QQ-A-250/5	T3	67.0	26.5	0.012
4	Al. Aly Faced Honey-comb Panel	QQ-A-250/5	T3	67.0	12.0	0.025
5	Al. Aly	QQ-A-250/5	T3	57.0	36.0	0.032
6	Al. Aly	QQ-A-250/5	T42	26.5	24.0	0.050
7	Al. Aly	QQ-A-250/5	T3	27.0	25.0	0.050
8	Al. Aly	QQ-A-250/5	T3	98.0	25.0	0.032
9	Al. Aly	QQ-A-250/5	T3	98.0	25.0	0.032
10	Al. Aly	QQ-A-250/5	T3	60.0	24.0	0.032
11	Al. Aly	QQ-A-250/5	T3	66.0	31.0	0.025
12	Al. Aly	QQ-A-250/5	T3	66.0	31.0	0.040
13	Al. Aly	QQ-A-250/5	T3	66.0	40.0	0.025
14	Al. Aly	QQ-A-250/5	T3	46.0	36.0	0.020
15	Al. Aly	QQ-A-250/5	T3	46.0	36.0	0.040
16	Al. Aly	QQ-A-250/5	T3	86.0	40.0	0.025
17	Al. Aly	QQ-A-250/5	T3	36.0	22.0	0.032
18	Al. Aly	QQ-A-250/5	T3	36.0	22.0	0.032

(a) Skin Panel Dimensions

Figure 4. UH-1B Tail Boom Skin Specifications

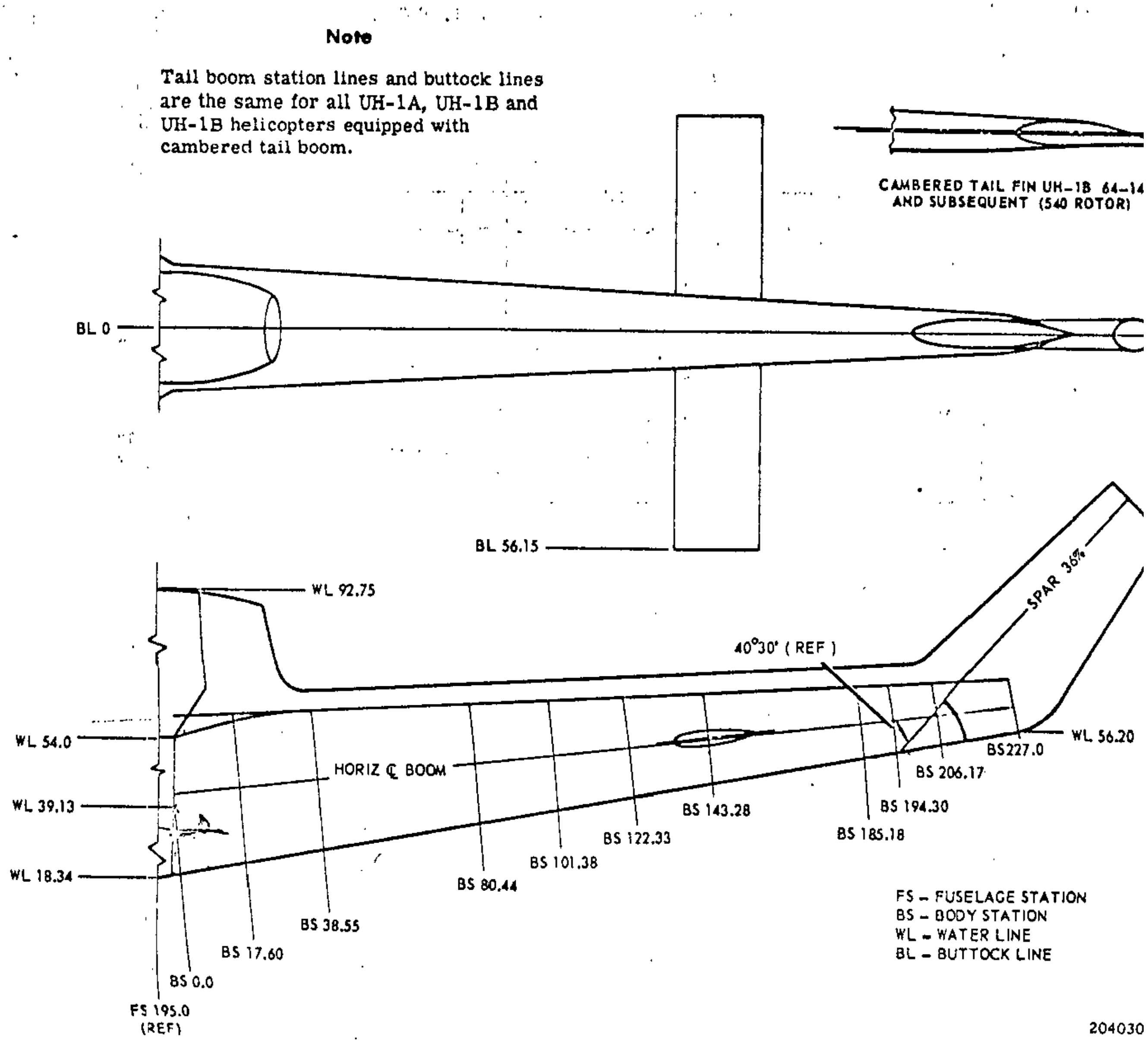

(b) Tail Boom Stations

Figure 4. Concluded

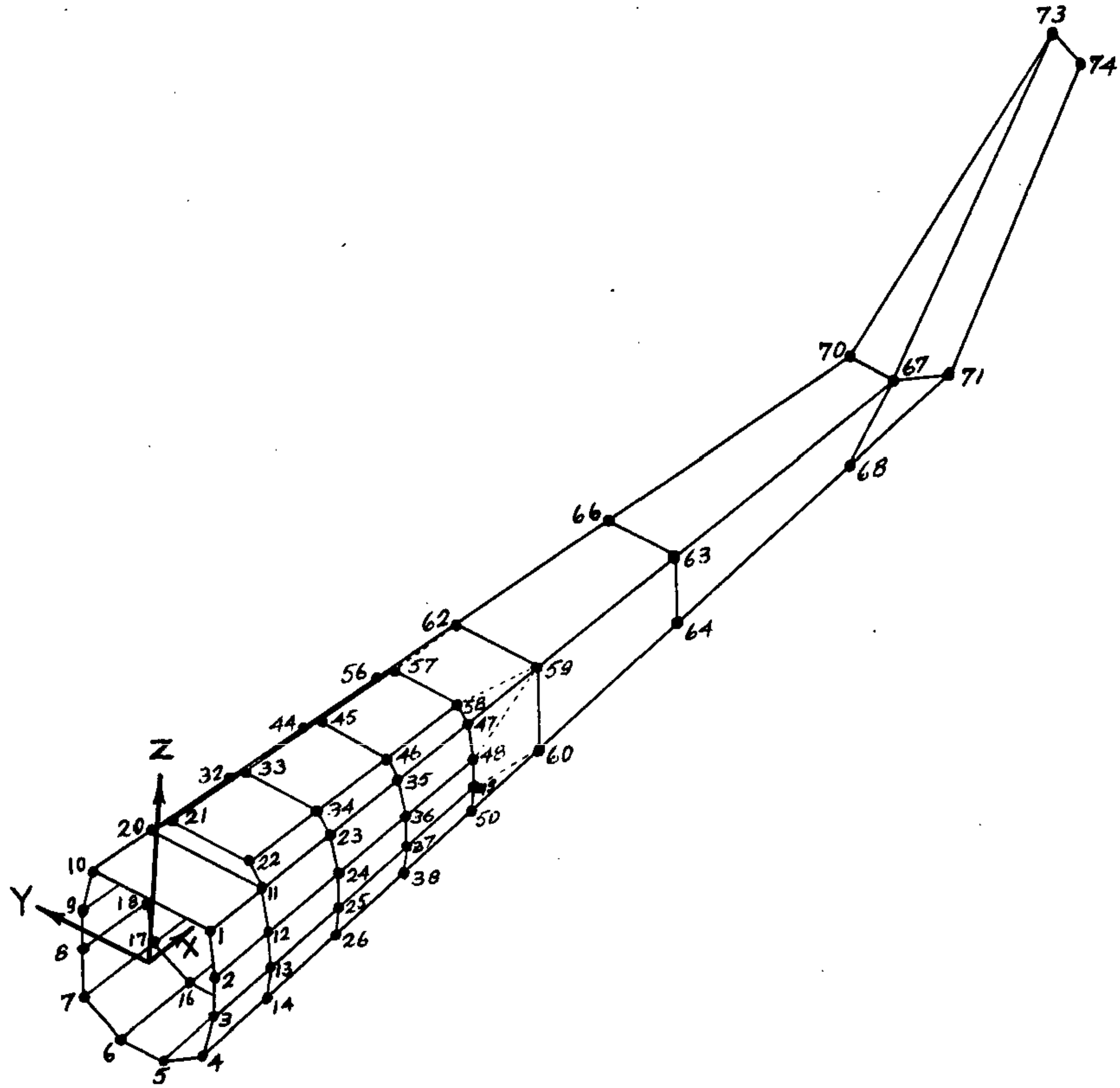

Figure 5. UH-1B Tail Boom Model Grid Points and Numbering Sequence

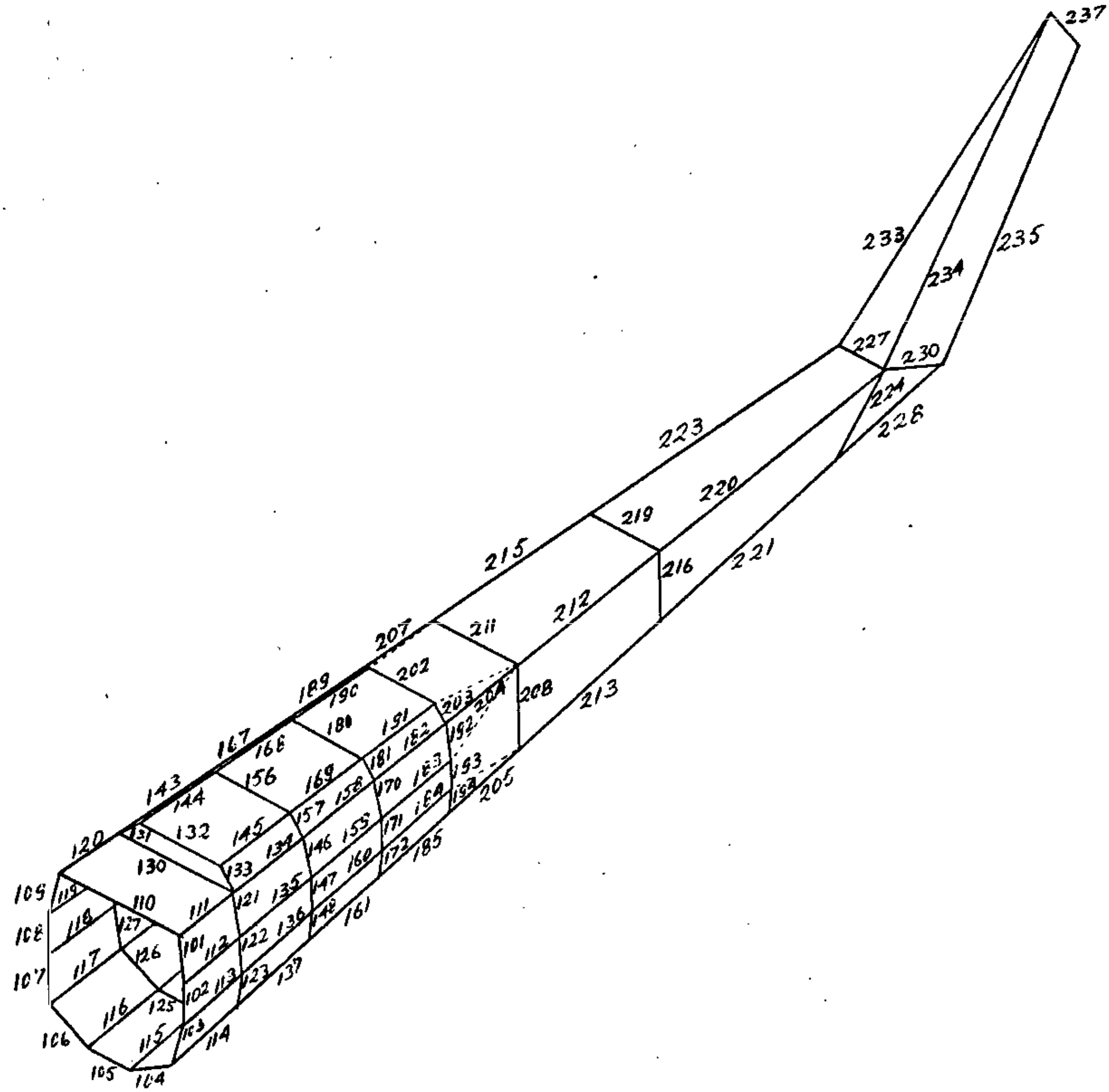

Figure 6. UH-1B Tail Boom Model Beam Element Identification

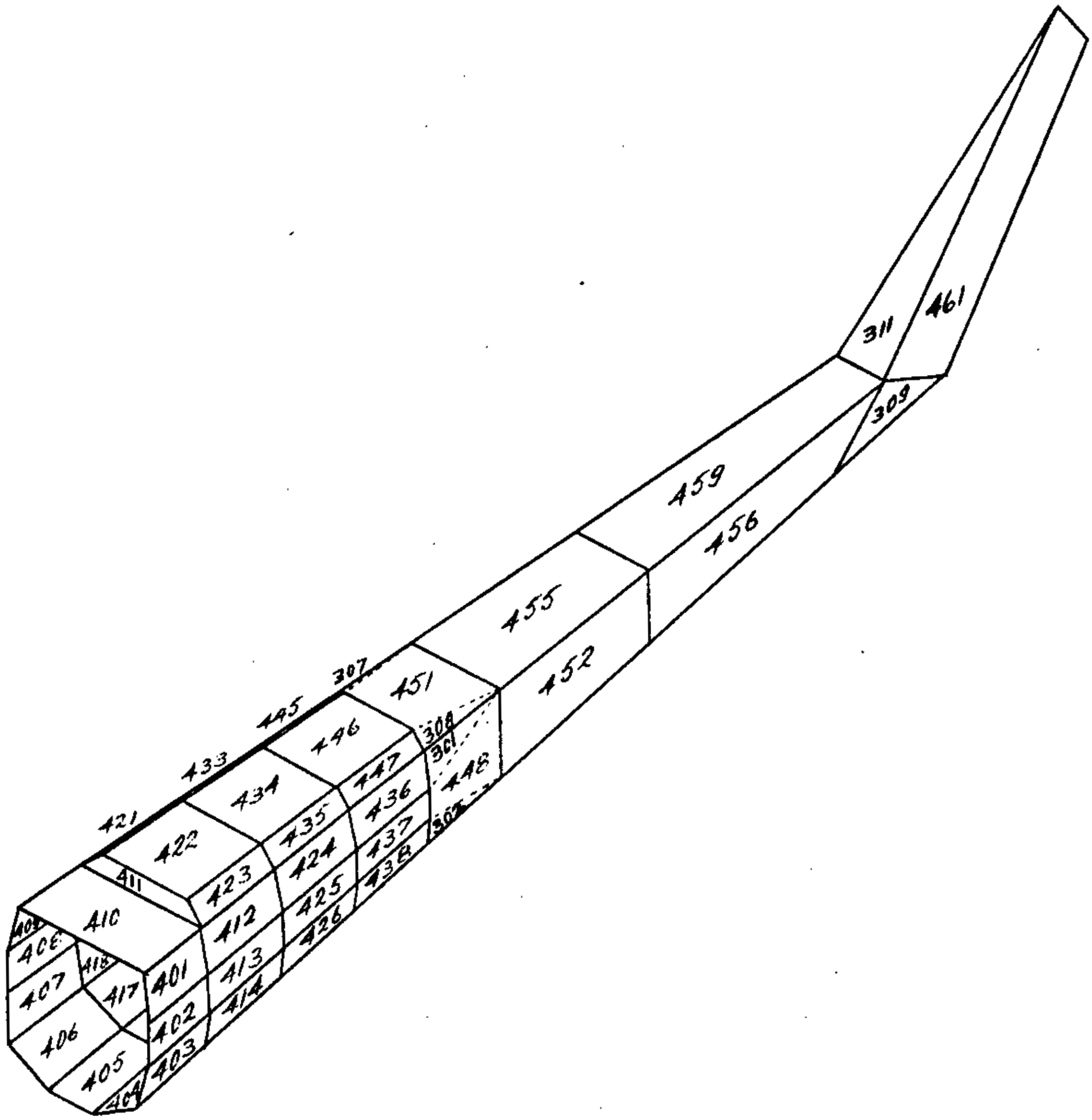

Figure 7. UH-1B Tail Boom Model Plate Element Identification

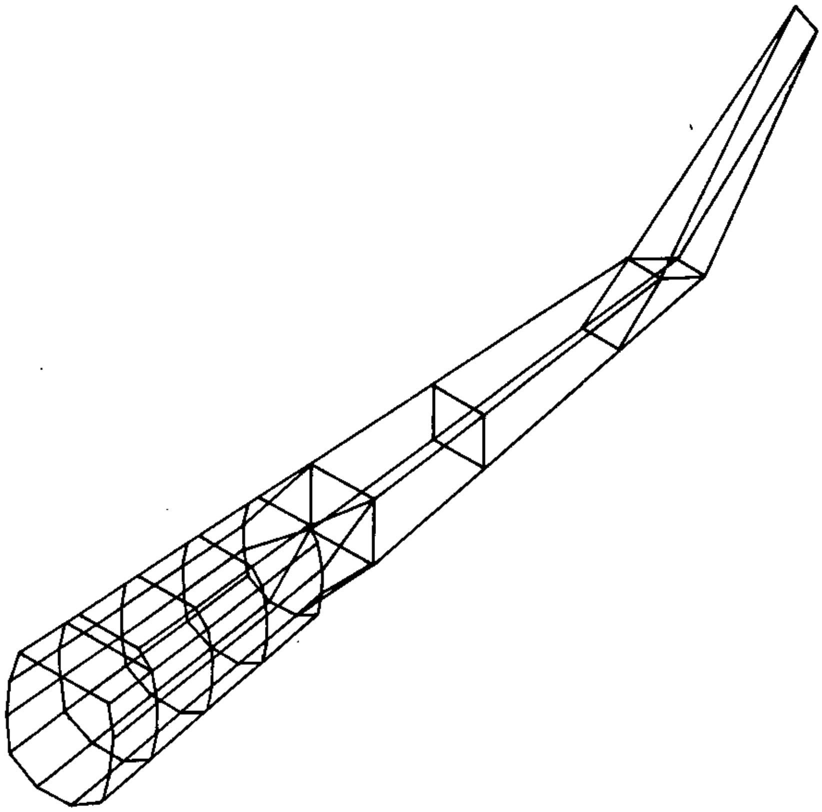

(a) Undeformed Model

Figure 8. UH-1B Tail Boom Model Bending Mode Shapes

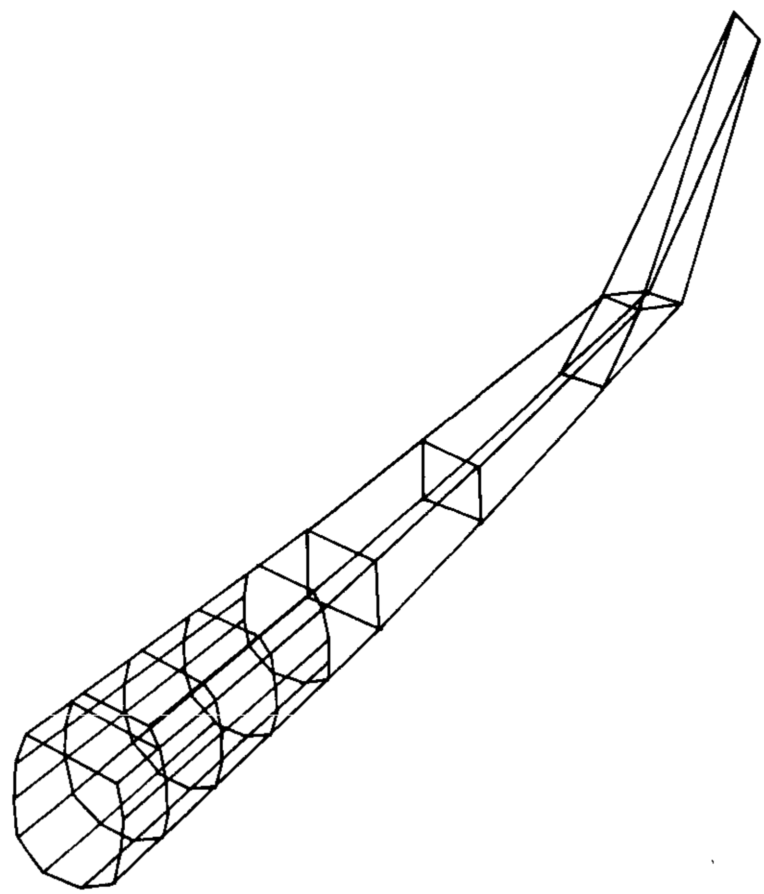

(b) Mode = 1, Frequency = 12.5 Hz

Figure 8. Continued

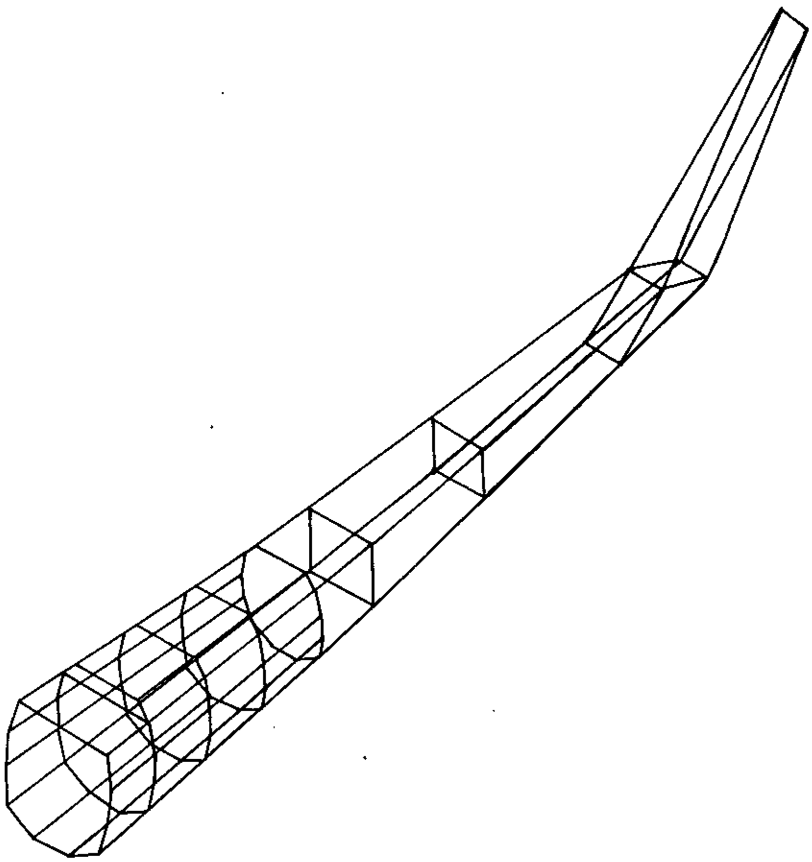

(c) Mode = 2, Frequency = 13.6 Hz

Figure 8. Continued

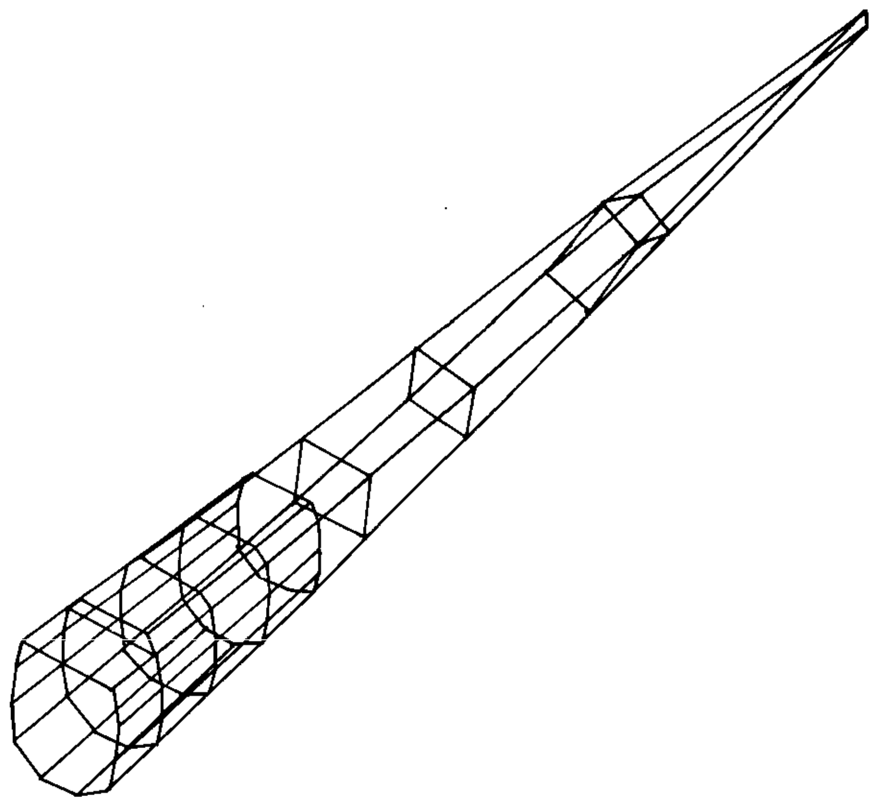

(d) Mode = 3, Frequency = 31.9 Hz.

Figure 8. Continued

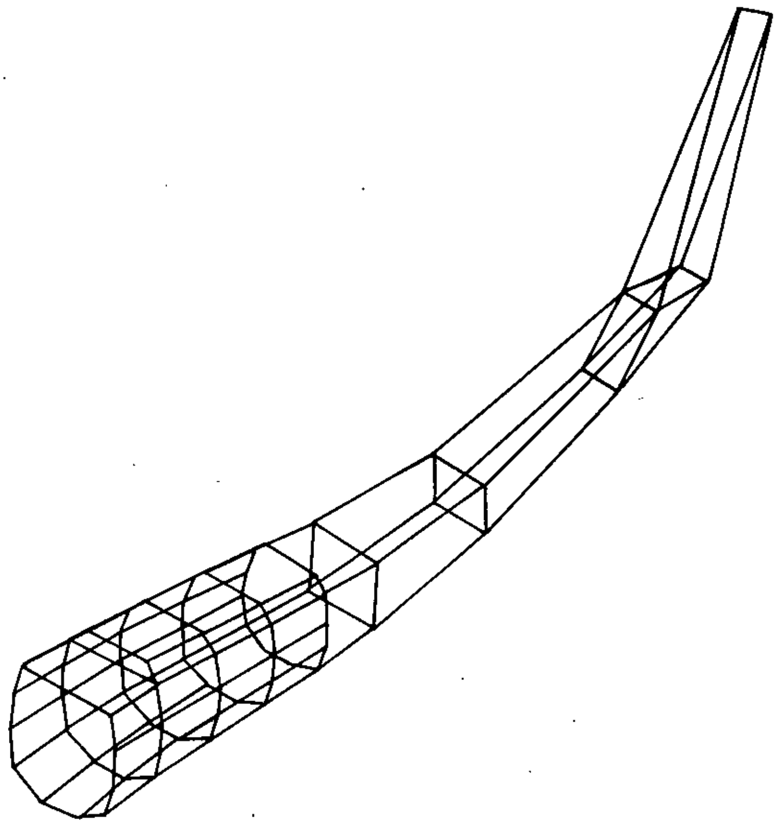

(e) Mode = 4, Frequency = 66.0 Hz.

Figure 8. Continued

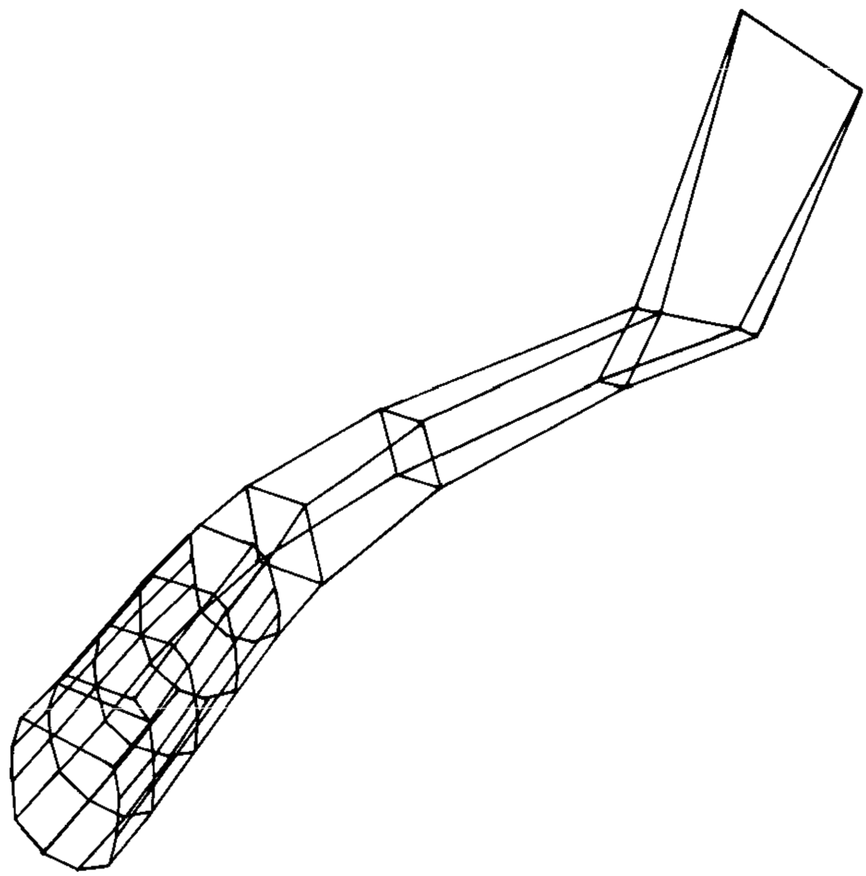

(f) Mode = 5, Frequency = 79.8 Hz.

Figure 8. Concluded

TABLE 1. CALCULATION OF CROSS-SECTION PROPERTIES FOR UH-1B STRINGER AND LONGERON

SEGMENT	b	h	R	$A_{circ\ segm.}$	A	half-circ. x_{cg}	x_{cg}	half-circ. y_{cg}	y_{cg}	$M_{x\ circ\ segm}$	M_x	$M_{y\ circ\ segm}$	M_y	$I_{half\text{-}circ.}$ I_{circ}*	$I_{xx\ N.A.}$	$I_{xx\ shift}$	$I_{xx\ TOT}$	$I_{yy\ N.A.}$	$I_{yy\ shift}$	$I_{yy\ TOT}$	$I_{xy\ circ.}$	I_{xy}	$J_{TORSION}$	Shear K_x	Shear K_y
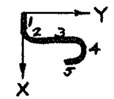				$\frac{1}{n}\pi R^2$	bxh	$\frac{4R}{3\pi}$	$\frac{b}{2}$	$\frac{4R}{3\pi}$	$\frac{h}{2}$	A y_{cg}	A y_{cg}	A x_{cg}	A x_{cg}	$0.1098R^4$ $\frac{\pi}{4}R^4$*	$\frac{bh^3}{12}$ +	$A(c_y-y_{cg})^2$	= Sum	$\frac{hb^3}{12}$ +	$A(c_x-x_{cg})^2$	= sum		A (c_y-y_{cg}) (c_x-x_{cg})	$\frac{Ut^3}{3}$ U=med. leng. t=thick	$\frac{A_x}{A_{TOT}}$	$\frac{A_y}{A_{TOT}}$
STRINGER																							or,		
1 FLANGE	0.628	0.032			0.020096		0.314		0.016		0.000322		0.006310		0.000002	0.001821	0.001823	0.000660	0.001869	0.002529		0.001845	$\frac{At^2}{3}$	(A_x + A_y = A_{TOT})	
2 OUT FILLET			0.122	0.011690		0.679778		0.070222		0.000821		0.007947		0.000012		(0.00712)			(0.000043)		-0.000175		where A=area		
2 IN FILLET			0.090	0.006362		0.666197		0.083803		0.000533		0.004238		0.000004		- (0.000346)			- (0.000014)		- -0.000070		t=thick. (for		
2 NET FILLET			(0.032)	net →	0.005328					net →	0.000288	net →	0.003709	net →	0.000008	= 0.000366	0.000344	0.000008	= 0.000029	0.000037	net →	-0.000105	open tube)		
3 STEM	0.032	0.541			0.017312		0.734		0.3925		0.006795		0.012707		0.000422	0.000099	0.000521	0.000001	0.000229	0.000230		0.000150			
4 OUT CIRC.			0.152	0.036292		cent.		0.727511		0.026403		-		0.000059		(0.006116)					0.003739				
4 IN CIRC.			0.120	0.022619		cent.		0.713930						0.000210*		-					- 0.002254				
4 NET CIRC.			(0.032)	net →	0.013673	→	0.870			0.016148		-		0.000023		(0.003564)		0.000129	0.000861	0.000990	net →	0.001485		(0.75+ 0.24) x(0.032) ÷A_{TOT} =	(0.815) x(0.032) ÷A_{TOT} =
5 TIP	0.032	0.023			0.000736		1.006		0.6515					0.000081*		=		0.000000	0.000110	0.000110		0.000095			
					A=0.057145in²					net →	0.010255	→	0.011896	net →	0.000036	0.002552	0.002588								
											0.000480		0.000740		0.000000	0.000082	0.000082			I_{yy} 0.003896in⁴		I_{xy}=0.003470in⁴	J=0.000020	K_x=0.55	K_y=0.45
LONGERON											0.018140		0.035362				I_{xx}= 0.005358in⁴	0.000468	0.026672	0.027140			$\frac{4A^2t}{U}$		
1 FLANGE	0.560	0.032			0.017920		1.220		0.016		÷A= C_y=0.317 in.		÷A= C_x=0.619 in.						(0.027690)				(for		
2 OUT FILLET			0.222	0.038708		0.845780		0.127780			0.000287	FOR WHOLE LONGERON,			0.000002	0.007249	0.007251		- (0.020939)				closed tube)		
2 IN FILLET			0.190	0.028353		0.859361		0.141361		0.004946				0.000133		(0.010638)		0.000061	= 0.006751	0.006812			A=mean area		
2 NET FILLET			(0.032)	net →	0.010355					0.004008				0.000072		- (0.007393)		0.000002	0.010951	0.010953			enclosed		
3 STEM	0.032	0.815			0.026080		0.648		0.620	net →	0.000938	M_y=0		net →	0.000061	= 0.003244	0.003305						$=(\frac{1.50+1.032}{2})$ x(1.55-0.532)		
4 OUT CIRC.			0.532	0.222287		TAKE WHOLE HALF-CIRCLE		1.243788			0.016170	DUE TO SYMMETRY.			0.001444	0.000027	0.001471	WHOLE HALF-CIRCLE		x 1/2 =			$+(\frac{1}{2}\pi\ 0.516^2)$		
4 IN CIRC.			0.500	0.196350				1.230207		0.276478				0.004398		- (0.077848)		0.006912	0.000000	0.003456			=1.707in² U=1.50+	(0.75 +0.50	(1.55 +1.55)
4 NET CIRC.			(0.032)	net →	0.025937	→	0.000					N.A. LIES ON Y-AXIS.		0.031456*						0.048361		SYMMETRY	2(0.815+0.222) +π 0.516 =5.195 in	+0.75) x0.032 ÷ A_{TOT} =	x0.032 ÷ A_{TOT} =
					0.080292 x 2 =					0.241551				0.003439* 0.024544*		= (0.065644)				x 2=					
					A=0.160584in²					net →	0.034927			net →	0.000959	0.012204	0.013163			I_{yy} = 0.096722in⁴		I_{xy}=0.0in⁴	J=0.071795in⁴	K_x=0.40	K_y=0.60
											0.052322	C_x = 0.000in.					0.025190						(For open tube J=0.000057in⁴)		
											x 2 ÷ A= C_y=0.652in.						x 2= I_{xx}=0.050380in.⁴								

TABLE 2. CALCULATION OF CROSS-SECTION PROPERTIES FOR UH-1B BULKHEAD FRAME

SEGMENT	b	h	A	x_{cg}	y_{cg}	M_x	M_y	$I_{xx_{NA}}$	$I_{xx_{SHIFT}}$	$I_{xx_{TOT}}$	$I_{yy_{NA}}$	$I_{yy_{SHIFT}}$	$I_{yy_{TOT}}$	I_{xy}	J_{TORS}	$K_{x_{SHEAR}}$	$K_{y_{SHEAR}}$
			bxh	$\frac{b}{2}$	$\frac{h}{2}$	Ay_{cg}	Ax_{cg}	$\frac{bh^3}{12}$	$+A(c_y-y_{cg})^2$	=sum	$\frac{hb^3}{12}$	$+A(c_x-x_{cg})^2$	= sum	$A(c_y-y_{cg})(c_x-x_{cg})$	$\frac{Ut^3}{3}$	$\frac{Ax}{A_{TOT}}$	$\frac{Ay}{A_{TOT}}$
1 TOP	0.359	0.032	0.011488	0.1795	2.718	0.031224	0.002062	0.000001	0.0025607	0.025608	0.000123	0.000096	0.000219	0.001569			
2 CENT	0.032	2.718	0.086976	0.000	1.359	0.118200	0.00	0.053545	0.001562	0.055107	0.000007	0.000674	0.000681	-0.001026			
3 BOTTOM	0.734	0.032	0.023488	0.367	0.000	0.00	0.008620	0.000002	0.035247	0.035249	0.001055	0.001828	0.002883	-0.008028			
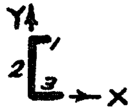			0.121952in^2			0.149424 ÷A= C_y=1.225	0.010682 ÷A= C_x=0.088			I_{xx}=0.115964in^4			I_{yy}=0.003783in^4	I_{xy}=-0.007485	0.000042in^4	0.29	0.71
CHECK SIMPLIFICATION:																	
1 TOP	0.5465	0.032	0.017488	0.27325	2.718	0.047532	0.004779	0.000001	0.032298	0.032298	0.000435	0.000667	0.001102	0.004640			
2 CENT	0.032	2.718	0.086976	0.000	1.359	0.118200	0.00	0.053545	0.00	0.053545	0.000007	0.000529	0.000536	0.00			
3 BOTTOM	0.5465	0.032	0.017488	0.27325	0.000	0.00	0.004779	0.000001	0.032298	0.032298	0.000435	0.000667	0.001102	-0.004640			
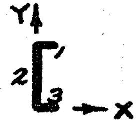			0.121952in^2			0.165732 ÷A= C_y=1.359	0.009558 ÷A= C_x=0.078			I_{xx}=0.118141in^4			I_{yy}=0.002740in^4	0.00	0.000042in^4	0.29	0.71
CHECK SIMPLIFICATION:																	
1 TOP	0.5625	0.032	0.018	0.00	1.359			0.000002	0.033244	0.033246	0.000475						
2 CENT	0.032	2.686	0.085952	0.00	0.00			0.051676	0.00	0.051676	0.000007						
3 BOTTOM	0.5625	0.032	0.018	0.00	-1.359			0.000002	0.033244	0.033246	0.000475						
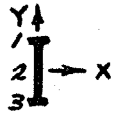			0.121952in^2			C_y=0.0	C_x=0.0			0.118768in^4			0.000957in^4	0.00	0.000042in^4	0.29	0.71

TABLE 3. UH-1B TAIL BOOM STRUCTURAL MASS COMPONENTS

GRID POINT	(INTERNAL POINT),	X = (in.)	Y = (in.)	Z = (in.)	MASS = ($lb\ sec^2/in.$)	
GRID POINT 1	(INTERNAL POINT 1),	0.15900E 1	-0.13950E 2	0.13850E 2	0.33786E -2	
GRID POINT 2	(INTERNAL POINT 2),	0.55000E 0	-0.15750E 2	0.47500E 1	0.16835E -2	@ X ≈ 0.0 in.
GRID POINT 3	(INTERNAL POINT 3),	-0.58000E 0	-0.15750E 2	-0.50500E 1	0.18117E -2	
GRID POINT 4	(INTERNAL POINT 4),	-0.16500E 1	-0.13950E 2	-0.14350E 2	0.19093E -2	
GRID POINT 5	(INTERNAL POINT 5),	-0.22600E 1	-0.52500E 1	-0.19700E 2	0.26837E -2	
GRID POINT 6	(INTERNAL POINT 6),	-0.22600E 1	0.52500E 1	-0.19700E 2	0.26837E -2	0.0229336 $\frac{lb\ sec^2}{in}$
GRID POINT 7	(INTERNAL POINT 7),	-0.16500E 1	0.13950E 2	-0.14350E 2	0.19093E -2	
GRID POINT 8	(INTERNAL POINT 8),	-0.58000E 0	0.15750E 2	-0.50500E 1	0.18117E -2	
GRID POINT 9	(INTERNAL POINT 9),	0.55000E 0	0.15750E 2	0.47500E 1	0.16835E -2	= 8.85 lbs.
GRID POINT 10	(INTERNAL POINT 10),	0.15900E 1	0.13950E 2	0.13850E 2	0.33786E -2	
GRID POINT 11	(INTERNAL POINT 11),	0.17600E 2	-0.13220E 2	0.13240E 2	0.27760E -2	
GRID POINT 12	(INTERNAL POINT 12),	0.17600E 2	-0.14940E 2	0.44700E 1	0.17647E -2	
GRID POINT 13	(INTERNAL POINT 13),	0.17600E 2	-0.14940E 2	-0.47100E 1	0.18984E -2	@ x = 17.6 in
GRID POINT 14	(INTERNAL POINT 14),	0.17600E 2	-0.13220E 2	-0.13500E 2	0.22340E -2	
GRID POINT 15	(INTERNAL POINT 15),	0.17600E 2	-0.49300E 1	-0.18600E 2	0.26883E -2	
GRID POINT 16	(INTERNAL POINT 16),	0.17600E 2	0.49300E 1	-0.18600E 2	0.26883E -2	
GRID POINT 17	(INTERNAL POINT 17),	0.17600E 2	0.13220E 2	-0.13500E 2	0.24640E -2	0.0276270 $\frac{lb\ sec^2}{in}$
GRID POINT 18	(INTERNAL POINT 18),	0.17600E 2	0.14940E 2	-0.47100E 1	0.23626E -2	
GRID POINT 19	(INTERNAL POINT 19),	0.17600E 2	0.14940E 2	0.44700E 1	0.22293E -2	
GRID POINT 20	(INTERNAL POINT 20),	0.17600E 2	0.13220E 2	0.13240E 2	0.30064E -2	= 10.66 lbs.
GRID POINT 21	(INTERNAL POINT 21),	0.17600E 2	0.94300E 1	0.17660E 2	0.17575E -2	
GRID POINT 22	(INTERNAL POINT 22),	0.17600E 2	-0.94300E 1	0.17660E 2	0.17575E -2	
GRID POINT 23	(INTERNAL POINT 23),	0.38550E 2	-0.12350E 2	0.12450E 2	0.17804E -2	
GRID POINT 24	(INTERNAL POINT 24),	0.38550E 2	-0.13980E 2	0.41200E 1	0.14450E -2	
GRID POINT 25	(INTERNAL POINT 25),	0.38550E 2	-0.13980E 2	-0.43200E 1	0.15149E -2	@ x = 38.55 in
GRID POINT 26	(INTERNAL POINT 26),	0.38550E 2	-0.12350E 2	-0.12570E 2	0.21013E -2	
GRID POINT 27	(INTERNAL POINT 27),	0.38550E 2	-0.46000E 1	-0.17280E 2	0.21744E -2	
GRID POINT 28	(INTERNAL POINT 28),	0.38550E 2	0.46000E 1	-0.17280E 2	0.21744E -2	
GRID POINT 29	(INTERNAL POINT 29),	0.38550E 2	0.12350E 2	-0.12570E 2	0.25423E -2	0.0253718 $\frac{lb\ sec^2}{ub}$
GRID POINT 30	(INTERNAL POINT 30),	0.38550E 2	0.13980E 2	-0.43200E 1	0.23984E -2	
GRID POINT 31	(INTERNAL POINT 31),	0.38550E 2	0.13980E 2	0.41200E 1	0.23325E -2	
GRID POINT 32	(INTERNAL POINT 32),	0.38550E 2	0.12350E 2	0.12450E 2	0.22254E -2	= 9.79 lbs.
GRID POINT 33	(INTERNAL POINT 33),	0.38550E 2	0.88500E 1	0.16520E 2	0.23414E -2	
GRID POINT 34	(INTERNAL POINT 34),	0.38550E 2	-0.88500E 1	0.16520E 2	0.23414E -2	
GRID POINT 35	(INTERNAL POINT 35),	0.59500E 2	-0.11490E 2	0.11650E 2	0.17705E -2	
GRID POINT 36	(INTERNAL POINT 36),	0.59500E 2	-0.13010E 2	0.37700E 1	0.14640E -2	
GRID POINT 37	(INTERNAL POINT 37),	0.59500E 2	-0.13010E 2	-0.39300E 1	0.14520E -2	@ x = 59.5 in
GRID POINT 38	(INTERNAL POINT 38),	0.59500E 2	-0.11490E 2	-0.11650E 2	0.20499E -2	
GRID POINT 39	(INTERNAL POINT 39),	0.59500E 2	-0.42600E 1	-0.15970E 2	0.20434E -2	
GRID POINT 40	(INTERNAL POINT 40),	0.59500E 2	0.42600E 1	-0.15970E 2	0.20434E -2	
GRID POINT 41	(INTERNAL POINT 41),	0.59500E 2	0.11490E 2	-0.11650E 2	0.24120E -2	0.0232376 $\frac{lb\ sec^2}{in}$
GRID POINT 42	(INTERNAL POINT 42),	0.59500E 2	0.13010E 2	-0.39300E 1	0.21689E -2	
GRID POINT 43	(INTERNAL POINT 43),	0.59500E 2	0.13010E 2	0.37700E 1	0.21881E -2	= 8.97 lbs.
GRID POINT 44	(INTERNAL POINT 44),	0.59500E 2	0.11490E 2	0.11650E 2	0.21398E -2	
GRID POINT 45	(INTERNAL POINT 45),	0.59500E 2	0.82700E 1	0.15380E 2	0.17528E -2	
GRID POINT 46	(INTERNAL POINT 46),	0.59500E 2	-0.82700E 1	0.15380E 2	0.17528E -2	

GRID POINT 47	(INTERNAL POINT 47),	X = 0.80440E 2	Y = -0.10620E 2	Z = 0.10860E 2	MASS = 0.19432E -2
GRID POINT 48	(INTERNAL POINT 48),	X = 0.80440E 2	Y = -0.12050E 2	Z = 0.34200E 1	MASS = 0.13965E -2
GRID POINT 49	(INTERNAL POINT 49),	X = 0.80440E 2	Y = -0.12050E 2	Z = -0.35400E 1	MASS = 0.13798E -2
GRID POINT 50	(INTERNAL POINT 50),	X = 0.80440E 2	Y = -0.10620E 2	Z = -0.10720E 2	MASS = 0.22130E -2
GRID POINT 51	(INTERNAL POINT 51),	X = 0.80440E 2	Y = -0.39300E 1	Z = -0.14800E 2	MASS = 0.13335E -2
GRID POINT 52	(INTERNAL POINT 52),	X = 0.80440E 2	Y = 0.39300E 1	Z = -0.14800E 2	MASS = 0.13335E -2
GRID POINT 53	(INTERNAL POINT 53),	X = 0.80440E 2	Y = 0.10620E 2	Z = -0.10720E 2	MASS = 0.24564E -2
GRID POINT 54	(INTERNAL POINT 54),	X = 0.80440E 2	Y = 0.12050E 2	Z = -0.35400E 1	MASS = 0.19872E -2
GRID POINT 55	(INTERNAL POINT 55),	X = 0.80440E 2	Y = 0.12050E 2	Z = 0.34200E 1	MASS = 0.20116E -2
GRID POINT 56	(INTERNAL POINT 56),	X = 0.80440E 2	Y = 0.10620E 2	Z = 0.10860E 2	MASS = 0.21943E -2
GRID POINT 57	(INTERNAL POINT 57),	X = 0.80440E 2	Y = 0.77000E 1	Z = 0.14250E 2	MASS = 0.15135E -2
GRID POINT 58	(INTERNAL POINT 58),	X = 0.80440E 2	Y = -0.77000E 1	Z = 0.14250E 2	MASS = 0.15135E -2
GRID POINT 59	(INTERNAL POINT 59),	X = 0.10138E 3	Y = -0.97500E 1	Z = 0.10060E 2	MASS = 0.71110E -2
GRID POINT 60	(INTERNAL POINT 60),	X = 0.10138E 3	Y = -0.97500E 1	Z = -0.98000E 1	MASS = 0.72407E -2
GRID POINT 61	(INTERNAL POINT 61),	X = 0.10138E 3	Y = 0.97500E 1	Z = -0.98000E 1	MASS = 0.76439E -2
GRID POINT 62	(INTERNAL POINT 62),	X = 0.10138E 3	Y = 0.97500E 1	Z = 0.10060E 2	MASS = 0.75175E -2
GRID POINT 63	(INTERNAL POINT 63),	X = 0.14328E 3	Y = -0.80200E 1	Z = 0.84800E 1	MASS = 0.11305E -1
GRID POINT 64	(INTERNAL POINT 64),	X = 0.14328E 3	Y = -0.80200E 1	Z = -0.79500E 1	MASS = 0.10262E -1
GRID POINT 65	(INTERNAL POINT 65),	X = 0.14328E 3	Y = 0.80200E 1	Z = -0.79500E 1	MASS = 0.10262E -1
GRID POINT 66	(INTERNAL POINT 66),	X = 0.14328E 3	Y = 0.80200E 1	Z = 0.84800E 1	MASS = 0.11305E -1
GRID POINT 67	(INTERNAL POINT 67),	X = 0.21000E 3	Y = -0.52600E 1	Z = 0.59500E 1	MASS = 0.20979E -1
GRID POINT 68	(INTERNAL POINT 68),	X = 0.19430E 3	Y = -0.59100E 1	Z = -0.57000E 1	MASS = 0.78695E -2
GRID POINT 69	(INTERNAL POINT 69),	X = 0.19430E 3	Y = 0.59100E 1	Z = -0.57000E 1	MASS = 0.78695E -2
GRID POINT 70	(INTERNAL POINT 70),	X = 0.21000E 3	Y = 0.52600E 1	Z = 0.59500E 1	MASS = 0.20979E -1
GRID POINT 71	(INTERNAL POINT 71),	X = 0.22700E 3	Y = -0.45600E 1	Z = -0.42500E 1	MASS = 0.14649E -1
GRID POINT 72	(INTERNAL POINT 72),	X = 0.22700E 3	Y = 0.45600E 1	Z = -0.42500E 1	MASS = 0.14649E -1
GRID POINT 73	(INTERNAL POINT 73),	X = 0.26300E 3	Y = 0.00000E 0	Z = 0.51000E 2	MASS = 0.27398E -1
GRID POINT 74	(INTERNAL POINT 74),	X = 0.27100E 3	Y = 0.00000E 0	Z = 0.37970E 2	MASS = 0.24486E -1

@ X = 80.44 in

$0.0212760 \frac{\text{lb sec}^2}{\text{in}}$

= 8.21 lbs.

@ X = 101.38 in

$0.0295131 \frac{\text{lb sec}^2}{\text{in}}$

= 11.39 lbs.

@ X = 143.28 in

$0.0431340 \frac{\text{lb sec}^2}{\text{in}}$

= 16.65

@ Tail Fin

$0.1388790 \frac{\text{lb sec}^2}{\text{in}}$

= 53.61 lb

CGMASS = 0.33197E 0 LOCATION X = 0.13882E 3 Y = 0.33344E 0 Z = 0.68333E 1

* * * * * NORMAL END OF JOB. * * * * *

lb sec^2/in

= 128 lbs.

TOTAL = $0.3319721 \frac{\text{lb sec}^2}{\text{in}}$

= 128 lbs.

TABLE 4. UH-1B TAIL BOOM TOTAL MASS COMPONENTS

		X (in.)	Y (in.)	Z (in.)	MASS ($lb\ sec^2/in$)
GRID POINT 1	(INTERNAL POINT 1),	0.15900E 1	-0.13950E 2	0.13850E 2	0.46786E -2
GRID POINT 2	(INTERNAL POINT 2),	0.55000E 0	-0.15750E 2	0.47500E 1	0.16835E -2
GRID POINT 3	(INTERNAL POINT 3),	-0.58000E 0	-0.15750E 2	-0.50500E 1	0.18117E -2
GRID POINT 4	(INTERNAL POINT 4),	-0.16500E 1	-0.13950E 2	-0.14350E 2	0.32093E -2
GRID POINT 5	(INTERNAL POINT 5),	-0.22600E 1	-0.52500E 1	-0.19700E 2	0.26837E -2
GRID POINT 6	(INTERNAL POINT 6),	-0.22600E 1	0.52500E 1	-0.19700E 2	0.26837E -2
GRID POINT 7	(INTERNAL POINT 7),	-0.16500E 1	0.13950E 2	-0.14350E 2	0.32093E -2
GRID POINT 8	(INTERNAL POINT 8),	-0.58000E 0	0.15750E 2	-0.50500E 1	0.18117E -2
GRID POINT 9	(INTERNAL POINT 9),	0.55000E 0	0.15750E 2	0.47500E 1	0.16835E -2
GRID POINT 10	(INTERNAL POINT 10),	0.15900E 1	0.13950E 2	0.13850E 2	0.46786E -2
GRID POINT 11	(INTERNAL POINT 11),	0.17600E 2	-0.13220E 2	0.13240E 2	0.55760E -2
GRID POINT 12	(INTERNAL POINT 12),	0.17600E 2	-0.14940E 2	0.44700E 1	0.17647E -2
GRID POINT 13	(INTERNAL POINT 13),	0.17600E 2	-0.14940E 2	-0.47100E 1	0.18984E -2
GRID POINT 14	(INTERNAL POINT 14),	0.17600E 2	-0.13220E 2	-0.13500E 2	0.50340E -2
GRID POINT 15	(INTERNAL POINT 15),	0.17600E 2	-0.49300E 1	-0.18600E 2	0.26883E -2
GRID POINT 16	(INTERNAL POINT 16),	0.17600E 2	0.49300E 1	-0.18600E 2	0.26883E -2
GRID POINT 17	(INTERNAL POINT 17),	0.17600E 2	0.13220E 2	-0.13500E 2	0.52640E -2
GRID POINT 18	(INTERNAL POINT 18),	0.17600E 2	0.14940E 2	-0.47100E 1	0.23626E -2
GRID POINT 19	(INTERNAL POINT 19),	0.17600E 2	0.14940E 2	0.44700E 1	0.22293E -2
GRID POINT 20	(INTERNAL POINT 20),	0.17600E 2	0.13220E 2	0.13240E 2	0.58064E -2
GRID POINT 21	(INTERNAL POINT 21),	0.17600E 2	0.94300E 1	0.17660E 2	0.17575E -2
GRID POINT 22	(INTERNAL POINT 22),	0.17600E 2	-0.94300E 1	0.17660E 2	0.17575E -2
GRID POINT 23	(INTERNAL POINT 23),	0.38550E 2	-0.12350E 2	0.12450E 2	0.48804E -2
GRID POINT 24	(INTERNAL POINT 24),	0.38550E 2	-0.13980E 2	0.41200E 1	0.14450E -2
GRID POINT 25	(INTERNAL POINT 25),	0.38550E 2	-0.13980E 2	-0.43200E 1	0.15149E -2
GRID POINT 26	(INTERNAL POINT 26),	0.38550E 2	-0.12350E 2	-0.12570E 2	0.52013E -2
GRID POINT 27	(INTERNAL POINT 27),	0.38550E 2	-0.46000E 1	-0.17280E 2	0.21744E -2
GRID POINT 28	(INTERNAL POINT 28),	0.38550E 2	0.46000E 1	-0.17280E 2	0.21744E -2
GRID POINT 29	(INTERNAL POINT 29),	0.38550E 2	0.12350E 2	-0.12570E 2	0.56423E -2
GRID POINT 30	(INTERNAL POINT 30),	0.38550E 2	0.13980E 2	-0.43200E 1	0.23984E -2
GRID POINT 31	(INTERNAL POINT 31),	0.38550E 2	0.13980E 2	0.41200E 1	0.23325E -2
GRID POINT 32	(INTERNAL POINT 32),	0.38550E 2	0.12350E 2	0.12450E 2	0.53254E -2
GRID POINT 33	(INTERNAL POINT 33),	0.38550E 2	0.88500E 1	0.16520E 2	0.23414E -2
GRID POINT 34	(INTERNAL POINT 34),	0.38550E 2	-0.88500E 1	0.16520E 2	0.23414E -2
GRID POINT 35	(INTERNAL POINT 35),	0.59500E 2	-0.11490E 2	0.11650E 2	0.48705E -2
GRID POINT 36	(INTERNAL POINT 36),	0.59500E 2	-0.13010E 2	0.37700E 1	0.14640E -2
GRID POINT 37	(INTERNAL POINT 37),	0.59500E 2	-0.13010E 2	-0.39300E 1	0.14520E -2
GRID POINT 38	(INTERNAL POINT 38),	0.59500E 2	-0.11490E 2	-0.11650E 2	0.51499E -2
GRID POINT 39	(INTERNAL POINT 39),	0.59500E 2	-0.42600E 1	-0.15970E 2	0.20434E -2
GRID POINT 40	(INTERNAL POINT 40),	0.59500E 2	0.42600E 1	-0.15970E 2	0.20434E -2
GRID POINT 41	(INTERNAL POINT 41),	0.59500E 2	0.11490E 2	-0.11650E 2	0.55120E -2
GRID POINT 42	(INTERNAL POINT 42),	0.59500E 2	0.13010E 2	-0.39300E 1	0.21689E -2
GRID POINT 43	(INTERNAL POINT 43),	0.59500E 2	0.13010E 2	0.37700E 1	0.21881E -2
GRID POINT 44	(INTERNAL POINT 44),	0.59500E 2	0.11490E 2	0.11650E 2	0.52398E -2
GRID POINT 45	(INTERNAL POINT 45),	0.59500E 2	0.82700E 1	0.15380E 2	0.17528E -2
GRID POINT 46	(INTERNAL POINT 46),	0.59500E 2	-0.82700E 1	0.15380E 2	0.17528E -2

```
GRID POINT  47 (INTERNAL POINT  47), X =   0.80440E  2 Y =  -0.10620E  2 Z =   0.10860E  2 MASS =   0.50432E -2
GRID POINT  48 (INTERNAL POINT  48), X =   0.80440E  2 Y =  -0.12050E  2 Z =   0.34200E  1 MASS =   0.13965E -2
GRID POINT  49 (INTERNAL POINT  49), X =   0.80440E  2 Y =  -0.12050E  2 Z =  -0.35400E  1 MASS =   0.13798E -2
GRID POINT  50 (INTERNAL POINT  50), X =   0.80440E  2 Y =  -0.10620E  2 Z =  -0.10720E  2 MASS =   0.53130E -2
GRID POINT  51 (INTERNAL POINT  51), X =   0.80440E  2 Y =  -0.39300E  1 Z =  -0.14800E  2 MASS =   0.13335E -2
GRID POINT  52 (INTERNAL POINT  52), X =   0.80440E  2 Y =   0.39300E  1 Z =  -0.14800E  2 MASS =   0.13335E -2
GRID POINT  53 (INTERNAL POINT  53), X =   0.80440E  2 Y =   0.10620E  2 Z =  -0.10720E  2 MASS =   0.55564E -2
GRID POINT  54 (INTERNAL POINT  54), X =   0.80440E  2 Y =   0.12050E  2 Z =  -0.35400E  1 MASS =   0.19872E -2
GRID POINT  55 (INTERNAL POINT  55), X =   0.80440E  2 Y =   0.12050E  2 Z =   0.34200E  1 MASS =   0.20116E -2
GRID POINT  56 (INTERNAL POINT  56), X =   0.80440E  2 Y =   0.10620E  2 Z =   0.10860E  2 MASS =   0.52943E -2
GRID POINT  57 (INTERNAL POINT  57), X =   0.80440E  2 Y =   0.77000E  1 Z =   0.14250E  2 MASS =   0.15135E -2
GRID POINT  58 (INTERNAL POINT  58), X =   0.80440E  2 Y =  -0.77000E  1 Z =   0.14250E  2 MASS =   0.15135E -2
GRID POINT  59 (INTERNAL POINT  59), X =   0.10138E  3 Y =  -0.97500E  1 Z =   0.10060E  2 MASS =   0.11711E -1
GRID POINT  60 (INTERNAL POINT  60), X =   0.10138E  3 Y =  -0.97500E  1 Z =  -0.98000E  1 MASS =   0.11841E -1
GRID POINT  61 (INTERNAL POINT  61), X =   0.10138E  3 Y =   0.97500E  1 Z =  -0.98000E  1 MASS =   0.12244E -1
GRID POINT  62 (INTERNAL POINT  62), X =   0.10138E  3 Y =   0.97500E  1 Z =   0.10060E  2 MASS =   0.12118E -1
GRID POINT  63 (INTERNAL POINT  63), X =   0.14328E  3 Y =  -0.80200E  1 Z =   0.84800E  1 MASS =   0.18205E -1
GRID POINT  64 (INTERNAL POINT  64), X =   0.14328E  3 Y =  -0.80200E  1 Z =  -0.79500E  1 MASS =   0.17162E -1
GRID POINT  65 (INTERNAL POINT  65), X =   0.14328E  3 Y =   0.80200E  1 Z =  -0.79500E  1 MASS =   0.17162E -1
GRID POINT  66 (INTERNAL POINT  66), X =   0.14328E  3 Y =   0.80200E  1 Z =   0.84800E  1 MASS =   0.18205E -1
GRID POINT  67 (INTERNAL POINT  67), X =   0.21000E  3 Y =  -0.52600E  1 Z =   0.59500E  1 MASS =   0.25779E -1
GRID POINT  68 (INTERNAL POINT  68), X =   0.19430E  3 Y =  -0.59100E  1 Z =  -0.57000E  1 MASS =   0.17769E -1
GRID POINT  69 (INTERNAL POINT  69), X =   0.19430E  3 Y =   0.59100E  1 Z =  -0.57000E  1 MASS =   0.17769E -1
GRID POINT  70 (INTERNAL POINT  70), X =   0.21000E  3 Y =   0.52600E  1 Z =   0.59500E  1 MASS =   0.25779E -1
GRID POINT  71 (INTERNAL POINT  71), X =   0.22700E  3 Y =  -0.45600E  1 Z =  -0.42500E  1 MASS =   0.17149E -1
GRID POINT  72 (INTERNAL POINT  72), X =   0.22700E  3 Y =   0.45600E  1 Z =  -0.42500E  1 MASS =   0.17149E -1
GRID POINT  73 (INTERNAL POINT  73), X =   0.26300E  3 Y =   0.00000E  0 Z =   0.51000E  2 MASS =   0.27398E -1
GRID POINT  74 (INTERNAL POINT  74), X =   0.27100E  3 Y =   0.00000E  0 Z =   0.37970E  2 MASS =   0.24486E -1

CGMASS =     0.46597E  0 LOCATION X =    0.13158E  3 Y =    0.23755E  0 Z =   0.47182E  1
                    * * * * * NORMAL END OF JOB. * * * * *
```

lb sec^2/in

= <u>180 lbs.</u>

```
ID UH18,DEC76
APP DISPLACEMENT
CHKPNT YES
SOL NORMAL MODES
TIME 100
ALTER 31
OUTPUT3 MGG,,,,//C,N,0/,C,N,XYZ $
ENDALTER
CEND
SPC=1
TITLE=UH18
MAXLINES=100000
METHOD=1
OUTPUT
DISPLACEMENT=ALL
OUTPUT(PLOT)
PLOTTER NASTPLT D 1
SET 91 = BAR
SET 92 = QUAD2
VIEW 140.0,40.0,0.0
FIND
PLOT LABEL GRID POINTS SET 91
PLOT SET 92
PLOT MODAL DEFORMATION SET 91
BEGIN BULK
GRID     1                 1.59     -13.95   13.85
GRID     2                 0.55     -15.75   4.75
GRID     3                 -0.58    -15.75   -5.05
GRID     4                 -1.65    -13.95   -14.35
GRID     5                 -2.26    -5.25    -19.70
GRID     6                 -2.26    5.25     -19.70
GRID     7                 -1.65    13.95    -14.35
GRID     8                 -0.58    15.75    -5.05
GRID     9                 0.55     15.75    4.75
GRID     10                1.59     13.95    13.85
GRID     11                17.60    -13.22   13.24
GRID     12                17.60    -14.94   4.47
GRID     13                17.60    -14.94   -4.71
GRID     14                17.60    -13.22   -13.50
GRID     15                17.60    -4.93    -18.60
GRID     16                17.60    4.93     -18.60
GRID     17                17.60    13.22    -13.50
GRID     18                17.60    14.94    -4.71
GRID     19                17.60    14.94    4.47
GRID     20                17.60    13.22    13.24
GRID     21                17.60    9.43     17.66
GRID     22                17.60    -9.43    17.66
GRID     23                38.55    -12.35   12.45
GRID     24                38.55    -13.98   4.12
GRID     25                38.55    -13.98   -4.32
GRID     26                38.55    -12.35   -12.57
GRID     27                38.55    -4.60    -17.28
GRID     28                38.55    4.60     -17.28
GRID     29                38.55    12.35    -12.57
GRID     30                38.55    13.98    -4.32
```

GRID	31		38.55	13.98	4.12	
GRID	32		38.55	12.35	12.45	
GRID	33		38.55	8.85	16.52	
GRID	34		38.55	-8.85	16.52	
GRID	35		59.50	-11.49	11.65	
GRID	36		59.50	-13.01	3.77	
GRID	37		59.50	-13.01	-3.93	
GRID	38		59.50	-11.49	-11.65	
GRID	39		59.50	-4.26	-15.97	
GRID	40		59.50	4.26	-15.97	
GRID	41		59.50	11.49	-11.65	
GRID	42		59.50	13.01	-3.93	
GRID	43		59.50	13.01	3.77	
GRID	44		59.50	11.49	11.65	
GRID	45		59.50	8.27	15.38	
GRID	46		59.50	-8.27	15.38	
GRID	47		80.44	-10.62	10.86	
GRID	48		80.44	-12.05	3.42	
GRID	49		80.44	-12.05	-3.54	
GRID	50		80.44	-10.62	-10.72	
GRID	51		80.44	-3.93	-14.80	
GRID	52		80.44	3.93	-14.80	
GRID	53		80.44	10.62	-10.72	
GRID	54		80.44	12.05	-3.54	
GRID	55		80.44	12.05	3.42	
GRID	56		80.44	10.62	10.86	
GRID	57		80.44	7.70	14.25	
GRID	58		80.44	-7.70	14.25	
GRID	59		101.38	-9.75	10.06	
GRID	60		101.38	-9.75	-9.80	
GRID	61		101.38	9.75	-9.80	
GRID	62		101.38	9.75	10.06	
GRID	63		143.28	-8.02	8.48	
GRID	64		143.28	-8.02	-7.95	
GRID	65		143.28	8.02	-7.95	
GRID	66		143.28	8.02	8.48	
GRID	67		210.00	-5.26	5.95	
GRID	68		194.30	-5.91	-5.70	
GRID	69		194.30	5.91	-5.70	
GRID	70		210.00	5.26	5.95	
GRID	71		227.00	-4.56	-4.25	
GRID	72		227.00	4.56	-4.25	
GRID	73		263.00	0.00	51.00	
GRID	74		271.00	0.00	37.97	
CBAR	101	14	1	2	11	2
CBAR	102	15	2	3	12	2
CBAR	103	16	3	4	13	2
CBAR	104	17	4	5	14	2
CBAR	105	18	5	6	15	2
CBAR	106	17	6	7	16	2
CBAR	107	16	7	8	17	2
CBAR	108	15	8	9	18	2
CBAR	109	14	9	10	19	2
CBAR	110	19	10	1	20	2

CBAR	111	20	1	11	0.0	0.392	0.920	1
CBAR	112	23	2	12	3			2
CBAR	113	23	3	13	2			2
CBAR	114	12	4	14	0.0	-0.392	0.920	1
CBAR	115	27	5	15	6			2
CBAR	116	27	6	16	5			2
CBAR	117	12	7	17	0.0	0.392	0.920	1
CBAR	118	23	8	18	9			2
CBAR	119	23	9	19	8			2
CBAR	120	20	10	20	0.0	-0.392	0.920	1
CBAR	121	13	11	12	23			2
CBAR	122	13	12	13	24			2
CBAR	123	13	13	14	25			2
CBAR	124	13	14	15	26			2
CBAR	125	13	15	16	27			2
CBAR	126	13	16	17	28			2
CBAR	127	13	17	18	29			2
CBAR	128	13	18	19	30			2
CBAR	129	13	19	20	31			2
CBAR	130	13	20	11	32			2
CBAR	131	13	20	21	32			2
CBAR	132	13	21	22	33			2
CBAR	133	13	22	11	34			2
CBAR	134	12	11	23	0.0	0.392	0.920	1
CBAR	135	11	12	24	13			2
CBAR	136	24	13	25	12			2
CBAR	137	20	14	26	0.0	-0.392	0.920	1
CBAR	138	11	15	27	16			2
CBAR	139	11	16	28	15			2
CBAR	140	20	17	29	0.0	0.392	0.920	1
CBAR	141	24	18	30	19			2
CBAR	142	11	19	31	18			2
CBAR	143	12	20	32	0.0	-0.392	0.920	1
CBAR	144	29	21	33	0.0	-0.866	0.500	1
CBAR	145	29	22	34	0.0	0.866	0.500	1
CBAR	146	13	23	24	35			2
CBAR	147	13	24	25	36			2
CBAR	148	13	25	26	37			2
CBAR	149	13	26	27	38			2
CBAR	150	13	27	28	39			2
CBAR	151	13	28	29	40			2
CBAR	152	13	29	30	41			2
CBAR	153	13	30	31	42			2
CBAR	154	13	31	32	43			2
CBAR	155	13	32	33	44			2
CBAR	156	13	33	34	45			2
CBAR	157	13	34	23	46			2
CBAR	158	12	23	35	0.0	0.392	0.920	1
CBAR	159	11	24	36	25			2
CBAR	160	11	25	37	24			2
CBAR	161	12	26	38	0.0	-0.392	0.920	1
CBAR	162	28	27	39	28			2
CBAR	163	28	28	40	27			2
CBAR	164	12	29	41	0.0	0.392	0.920	1
CBAR	165	11	30	42	31			2
CBAR	166	11	31	43	30			2

CBAR	167	12	32	44	0.0	-0.392	0.920	1
CBAR	168	11	33	45	0.0	-0.866	0.500	1
CBAR	169	11	34	46	0.0	0.866	0.500	1
CBAR	170	13	35	36	47			2
CBAR	171	13	36	37	48			2
CBAR	172	13	37	38	49			2
CBAR	173	13	38	39	50			2
CBAR	174	13	39	40	51			2
CBAR	175	13	40	41	52			2
CBAR	176	13	41	42	53			2
CBAR	177	13	42	43	54			2
CBAR	178	13	43	44	55			2
CBAR	179	13	44	45	56			2
CBAR	180	13	45	46	57			2
CBAR	181	13	46	35	58			2
CBAR	182	12	35	47	0.0	0.392	0.920	1
CBAR	183	11	36	48	37			2
CBAR	184	11	37	49	36			2
CBAR	185	12	38	50	0.0	-0.392	0.920	1
CBAR	186	12	41	53	0.0	0.392	0.920	1
CBAR	187	11	42	54	43			2
CBAR	188	11	43	55	42			2
CBAR	189	12	44	56	0.0	-0.392	0.920	1
CBAR	190	11	45	57	0.0	-0.866	0.500	1
CBAR	191	11	46	58	0.0	0.866	0.500	1
CBAR	192	13	47	48	59			2
CBAR	193	13	48	49	36			2
CBAR	194	13	49	50	37			2
CBAR	195	13	50	51	60			2
CBAR	196	13	51	52	39			2
CBAR	197	13	52	53	40			2
CBAR	198	13	53	54	61			2
CBAR	199	13	54	55	42			2
CBAR	200	13	55	56	43			2
CBAR	201	13	56	57	62			2
CBAR	202	13	57	58	45			2
CBAR	203	13	58	47	46			2
CBAR	204	22	47	59	0.0	0.392	0.920	1
CBAR	205	22	50	60	0.0	-0.392	0.920	1
CBAR	206	22	53	61	0.0	0.392	0.920	1
CBAR	207	22	56	62	0.0	-0.392	0.920	1
CBAR	208	25	59	60	63			2
CBAR	209	25	60	61	64			2
CBAR	210	25	61	62	65			2
CBAR	211	25	62	59	66			2
CBAR	212	21	59	63	0.0	0.392	0.920	1
CBAR	213	21	60	64	0.0	-0.392	0.920	1
CBAR	214	21	61	65	0.0	0.392	0.920	1
CBAR	215	21	62	66	0.0	-0.392	0.920	1
CBAR	216	26	63	64	67			2
CBAR	217	26	64	65	68			2
CBAR	218	26	65	66	69			2
CBAR	219	26	66	63	70			2
CBAR	220	21	63	67	0.0	0.392	0.920	1
CBAR	221	21	64	68	0.0	-0.392	0.920	1
CBAR	222	21	65	69	0.0	0.392	0.920	1
CBAR	223	21	66	70	0.0	-0.392	0.920	1

CBAR	224	26	67	68	71			2
CBAR	225	26	68	69	71			2
CBAR	226	26	69	70	72			2
CBAR	227	26	70	67	73			2
CBAR	228	21	68	71	0.0	-0.392	0.920	1
CBAR	229	21	69	72	0.0	0.392	0.920	1
CBAR	230	26	67	71	73			2
CBAR	231	26	71	72	74			2
CBAR	232	26	72	70	74			2
CBAR	233	30	70	73	72			2
CBAR	234	30	67	73	71			2
CBAR	235	30	71	74	67			2
CBAR	236	30	72	74	70			2
CBAR	237	30	73	74	70			2
CTRIA2	301	32	47	48	59	0.0		
CTRIA2	302	32	49	50	60	0.0		
CTRIA2	303	32	50	51	60	0.0		
CTRIA2	304	32	52	53	61	0.0		
CTRIA2	305	34	53	54	61	0.0		
CTRIA2	306	34	55	56	62	0.0		
CTRIA2	307	31	56	57	62	0.0		
CTRIA2	308	31	58	47	59	0.0		
CTRIA2	309	33	67	68	71	0.0		
CTRIA2	310	33	69	70	72	0.0		
CTRIA2	311	32	70	67	73	0.0		
CTRIA2	312	32	71	72	74	0.0		
CQUAD2	401	43	1	2	12	11	0.0	
CQUAD2	402	43	2	3	13	12	0.0	
CQUAD2	403	43	3	4	14	13	0.0	
CQUAD2	404	41	4	5	15	14	0.0	
CQUAD2	405	41	5	6	16	15	0.0	
CQUAD2	406	41	6	7	17	16	0.0	
CQUAD2	407	43	7	8	18	17	0.0	
CQUAD2	408	43	8	9	19	18	0.0	
CQUAD2	409	43	9	10	20	19	0.0	
CQUAD2	410	41	10	1	11	20	0.0	
CQUAD2	411	41	11	22	21	20	0.0	
CQUAD2	412	41	11	12	24	23	0.0	
CQUAD2	413	41	12	13	25	24	0.0	
CQUAD2	414	41	13	14	26	25	0.0	
CQUAD2	415	41	14	15	27	26	0.0	
CQUAD2	416	41	15	16	28	27	0.0	
CQUAD2	417	41	16	17	29	28	0.0	
CQUAD2	418	44	17	18	30	29	0.0	
CQUAD2	419	44	18	19	31	30	0.0	
CQUAD2	420	44	19	20	32	31	0.0	
CQUAD2	421	41	20	21	33	32	0.0	
CQUAD2	422	41	21	22	34	33	0.0	
CQUAD2	423	41	22	11	23	34	0.0	
CQUAD2	424	41	23	24	36	35	0.0	
CQUAD2	425	41	24	25	37	36	0.0	
CQUAD2	426	41	25	26	38	37	0.0	
CQUAD2	427	41	26	27	39	38	0.0	
CQUAD2	428	41	27	28	40	39	0.0	
CQUAD2	429	41	28	29	41	40	0.0	
CQUAD2	430	44	29	30	42	41	0.0	

CQUAD2	431	44	30	31	43	42	0.0
CQUAD2	432	44	31	32	44	43	0.0
CQUAD2	433	41	32	33	45	44	0.0
CQUAD2	434	41	33	34	46	45	0.0
CQUAD2	435	41	34	23	35	46	0.0
CQUAD2	436	42	35	36	48	47	0.0
CQUAD2	437	42	36	37	49	48	0.0
CQUAD2	438	42	37	38	50	49	0.0
CQUAD2	439	42	38	39	51	50	0.0
CQUAD2	440	42	39	40	52	51	0.0
CQUAD2	441	42	40	41	53	52	0.0
CQUAD2	442	44	41	42	54	53	0.0
CQUAD2	443	44	42	43	55	54	0.0
CQUAD2	444	44	43	44	56	55	0.0
CQUAD2	445	41	44	45	57	56	0.0
CQUAD2	446	41	45	46	58	57	0.0
CQUAD2	447	41	46	35	47	58	0.0
CQUAD2	448	42	48	49	60	59	0.0
CQUAD2	449	42	51	52	61	60	0.0
CQUAD2	450	44	54	55	62	61	0.0
CQUAD2	451	41	57	58	59	62	0.0
CQUAD2	452	43	59	60	64	63	0.0
CQUAD2	453	43	60	61	65	64	0.0
CQUAD2	454	43	61	62	66	65	0.0
CQUAD2	455	43	62	59	63	66	0.0
CQUAD2	456	44	63	64	68	67	0.0
CQUAD2	457	43	64	65	69	68	0.0
CQUAD2	458	44	65	66	70	69	0.0
CQUAD2	459	43	66	63	67	70	0.0
CQUAD2	460	43	68	69	72	71	0.0
CQUAD2	461	42	67	71	74	73	0.0
CQUAD2	462	42	72	70	73	74	0.0
PBAR	11	1	0.0571	0.0039	0.0054	0.00002	
PBAR	12	1	0.1606	0.0967	0.0504	0.07179	
PBAR	13	1	0.122	0.0038	0.116	0.00004	
PBAR	14	1	0.312	0.012	0.727	0.00026	
PBAR	15	1	0.352	0.012	1.119	0.00029	
PBAR	16	1	0.362	0.012	1.235	0.00030	
PBAR	17	1	0.387	0.012	1.555	0.00032	
PBAR	18	1	0.337	0.012	0.960	0.00028	
PBAR	19	1	0.512	0.012	3.947	0.00043	
PBAR	20	1	0.1892	0.0987	0.0531	0.07180	
PBAR	21	1	0.2177	0.1006	0.0558	0.07181	
PBAR	22	1	0.2748	0.1045	0.0612	0.07183	
PBAR	23	1	0.1142	0.0078	0.0108	0.00004	
PBAR	24	1	0.0857	0.0059	0.0081	0.00003	
PBAR	25	1	0.183	0.0057	0.174	0.00006	
PBAR	26	1	0.305	0.0095	0.290	0.00010	
PBAR	27	1	0.50	0.23	1.50	0.00042	
PBAR	28	1	0.30	0.0020	0.17	0.00013	
PBAR	29	1	0.24	0.0024	0.21	0.00004	
PBAR	30	1	1.2	7.2	7.2	0.1	

```
PTRIA2  31      2       0.020   0.0
PTRIA2  32      2       0.025   0.0
PTRIA2  33      2       0.032   0.0
PTRIA2  34      2       0.040   0.0
PQUAD2  41      2       0.020   0.0
PQUAD2  42      2       0.025   0.0
PQUAD2  43      2       0.032   0.0
PQUAD2  44      2       0.040   0.0
MAT1    1       10.3+6  3.96+6  0.3     0.00025 12.7-6  70.0
MAT1    2       10.6+6  4.08+6  0.3     0.00025 12.7-6  70.0
OMIT1   456     11      THRU    74
SPC1    1       123456  1       THRU    10
CONM2   501     1               0.0013
CONM2   502     4               0.0013
CONM2   503     7               0.0013
CONM2   504     10              0.0013
CONM2   505     11              0.0028
CONM2   506     14              0.0028
CONM2   507     17              0.0028
CONM2   508     20              0.0028
CONM2   509     23              0.0031
CONM2   510     26              0.0031
CONM2   511     29              0.0031
CONM2   512     32              0.0031
CONM2   513     35              0.0031
CONM2   514     38              0.0031
CONM2   515     41              0.0031
CONM2   516     44              0.0031
CONM2   517     47              0.0031
CONM2   518     50              0.0031
CONM2   519     53              0.0031
CONM2   520     56              0.0031
CONM2   521     59              0.0046
CONM2   522     60              0.0046
CONM2   523     61              0.0046
CONM2   524     62              0.0046
CONM2   525     63              0.0069
CONM2   526     64              0.0069
CONM2   527     65              0.0069
CONM2   528     66              0.0069
CONM2   529     68              0.0099
CONM2   530     69              0.0099
CONM2   531     67              0.0048
CONM2   532     70              0.0048
CONM2   533     71              0.0025
CONM2   534     72              0.0025
EIGR    1       GIV     0.0     30.0    10      10
+MSF1   MAX
ENDDATA
```

DISTRIBUTION LIST

No. of Copies	Organization
12	Commander Defense Documentation Center ATTN: DDC-TCA Cameron Station Alexandria, VA 22314
1	Commander US Army Materiel Development and Readiness Command ATTN: DRCDMA-ST 5001 Eisenhower Avenue Alexandria, VA 22333
1	Commander US Army Aviation Research and Development Command ATTN: DRSAV-E 12th and Spruce Streets St. Louis, MO 63166
1	Director US Army Air Mobility Research and Development Laboratory Ames Research Center Moffett Field, CA 94035
1	Director Eustis Directorate US Army Air Mobility Research and Development Laboratory ATTN: DAVDL-E-TAS, W. Figge Fort Eustis, VA 23604
1	Commander US Army Electronics Command ATTN: DRSEL-RD Fort Monmouth, NJ 07703
1	Commander US Army Missile Research and Development Command ATTN: DRDMI-R Redstone Arsenal, AL 35809
1	Commander US Army Tank Automotive Research & Development Cmd ATTN: DRDTA-RWL Warren, MI 48090
2	Commander US Army Mobility Equipment Research & Development Cmd ATTN: Tech Docu Cen, Bldg 315 DRSME-RZT Fort Belvoir, VA 22060
1	Commander US Army Armament Materiel Readiness Command ATTN: DRSAR-LEP-L, Tech Lib Rock Island, IL 61299
1	Commander US Army Harry Diamond Labs ATTN: DRXDO-NP 2800 Powder Mill Road Adelphi, MD 20783
1	Director US Army TRADOC Systems Analysis Activity ATTN: ATAA-SL, Tech Lib White Sands Missile Range NM 88002
1	Commander US Army Nuclear Agency ATTN: ACTN-W 7500 Backlick Rd., Bldg 2073 Springfield, VA 22150
1	AFWL/SAT, Mr. A. Sharp Kirtland AFB, NM 87117
2	Kaman Avidyne ATTN: Mr. Emanuel S. Criscione Northwest Industrial Park Burlington, MA 01803

DISTRIBUTION LIST

Aberdeen Proving Ground

Marine Corps Ln Ofc
Dir, USAMSAA